

The head morphology of the potentially basal heteropteran lineages Enicocephalomorpha and Dipsocoromorpha (Insecta: Hemiptera: Heteroptera)

RICO SPANGENBERG^{*,1}, KATRIN FRIEDEMANN¹, CHRISTIANE WEIRAUCH² & ROLF G. BEUTEL¹

¹ Institut für Spezielle Zoologie und Evolutionsbiologie mit Phyletischem Museum, FSU Jena, 07743 Jena, Germany; Rico Spangenberg* [rico.spangenberg@gmail.com] — ² Entomology, University of California, Riverside, CA 92521, U.S.A. — * Corresponding author

Accepted 13.ix.2013.

Published online at www.senckenberg.de/arthropod-systematics on 8.xi.2013.

Abstract

The systematic positions of Enicocephalomorpha and Dipsocoromorpha are still controversial and the available morphological information is very fragmentary. Consequently, head structures of *Cryptostemma* (Dipsocoromorpha: Dipsocoridae) and *Systelloderes* (Enicocephalomorpha: Enicocephalidae) were investigated in detail using SEM, serial sectioning and computer-based 3D-reconstruction. The observed features were compared to putatively homologous structures in Nepomorpha, Leptopodomorpha, Cimicomorpha, and Pentatomomorpha. A cladistic analysis based on 71 cephalic characters scored for 16 heteropteran terminals and outgroup taxa resulted in a strict consensus of two minimum length trees. The monophyly of Heteroptera is strongly supported. However, in the present study, the branching pattern within the group is not compatible with recent hypotheses (e.g., Nepomorpha paraphyletic herein). Characters of the head alone are not sufficient to reconstruct the basal branching events in Heteroptera. This is arguably due to homoplasy related to similar feeding habits. Consequently, we evaluated the cephalic characters based on previously published cladograms. A hypothesis with Enicocephalomorpha as the sister group of the remaining Heteroptera (Euheteroptera), followed by Dipsocoromorpha, required the lowest number of steps. Euheteroptera are supported by the presence of distinct bucculae, and Neoheteroptera (Euheteroptera excl. Dipsocoromorpha) by the presence of paired postoccipital condyles and distinctly bi-lobed principal salivary glands. A conspicuous autapomorphy of Enicocephalomorpha is the distinct constriction of the head capsule posterad of the compound eyes and probably also the elongation of the head and the presence of “scapus sclerites”. Dipsocoromorpha differ strongly from Enicocephalomorpha in their head morphology. Convincing cephalic autapomorphies are lacking. Gerromorpha are characterized by cephalic trichobothria originating in a deep pit and by a quadrangular mandibular lever.

Key words

Systelloderes, *Cryptostemma*, *Gerris*, musculature, nervous system, alimentary system, phylogeny, anatomy.

1. Introduction

Heteroptera or True Bugs are a megadiverse group of Hemiptera (>40.000) displaying remarkable morphological variation (e.g., SCHUH & SLATER 1995; HENRY 2009). Despite considerable efforts to reconstruct the phylogeny of the group for more than 30 years (see e.g., SCHUH & WEIRAUCH 2011), the higher-level systematics of Hetero-

ptera is clearly an issue of ongoing debate (see e.g., LI et al. 2012b). This controversy concerns in particular the respective positions of Enicocephalomorpha (unique-headed bugs), Dipsocoromorpha (minute litter bugs), Nepomorpha (aquatic bugs), and Gerromorpha (semi-aquatic bugs). The modern era of heteropteran classification

started in the 1950s with attempts to subdivide the polyphyletic Geocorisae, the terrestrial groups, recognized by earlier authors: LESTON et al. (1954) defined Pentatomomorpha (stink bugs and allies) and Cimicomorpha (assassin and plant bugs and relatives), but as other authors during this period they did not apply explicitly phylogenetic (Hennigian) approaches. MIYAMOTO (1961) subsequently suggested a basal position for the unique-headed bugs and the minute litter bugs based on the plesiomorphic condition of the alimentary system. He combined the “Dipsocoridae” and “Enicocephalidae” as “Dipsocoromorpha”, a group that was obviously based on symplesiomorphies and that he considered to be “parallel” to Cimicomorpha and Pentatomomorpha. ŠTYS & KERZHNER (1975) created the currently used scheme for the higher-level classification of Heteroptera in which they recognized 7 infraorders: Enicocephalomorpha Stichel, 1955; Dipsocoromorpha Miyamoto, 1961; Gerromorpha Popov, 1971; Nepomorpha Popov, 1968; Leptopodomorpha Popov, 1971; Cimicomorpha Leston, Pendergrast & Southwood, 1954 and Pentatomomorpha Leston, Pendergrast & Southwood, 1954. A phylogenetic evaluation of this scheme was beyond the scope of their publication.

Subsequent attempts to incorporate phylogenetic interpretation into the classification of Heteroptera were made by COBBEN (1968, 1978) in his seminal comparative morphological studies, although he emphasized that cladistic methods were unsuitable to reveal the phylogeny of true bugs due to the high degree of homoplasy within the group (reviewed by SCHUH 1979). COBBEN (1978) proposed Heteroptera to be derived from a “gerromorphan stock”, with different groups having evolved to different degrees from this ancestral assemblage. Based on this scheme, he considered Enicocephalomorpha and Dipsocoromorpha to be anagenetically close to the heteropteran ancestor and all other taxa to be more derived.

SCHUH (1979) re-analyzed Cobben’s data using explicit cladistic procedures. This analysis placed Enicocephalomorpha as the most basal heteropteran lineage with the complete branching pattern as follows: Enicocephalomorpha + (Dipsocoromorpha + (Gerromorpha + ((Leptopodomorpha + Nepomorpha) + (Cimicomorpha + Pentatomomorpha))))). A study based on 31 morphological characters and 669 base pairs of 18S rDNA (WHEELER et al. 1993) gave further support (at least in some of their analyses) to the phylogeny proposed by SCHUH (1979), and the concept of Enicocephalomorpha, Dipsocoromorpha and Gerromorpha as basal heteropteran lineages was also adopted by SWEET (1979), SCHUH & SLATER (1995), HENRY (2009), CASSIS & SCHUH (2010), and WEIRAUCH & SCHUH (2011) (see also CARVER et al. 1991 [Coleorrhyncha included as most basal branch]). In the cladograms of SCHUH (1979) and WHEELER et al. (1993), Heteroptera are subdivided into the following monophyletic clades: Enicocephalomorpha + Euheteroptera (ŠTYS 1983, 1984) (= Dipsocoromorpha + (Neoheteroptera (= Gerromorpha + (Panheteroptera (= Nepomorpha + (Leptopodomorpha + (Cimicomorpha + Pentatomomorpha)))))). However, the morphology-only analysis of WHEELER et al. (1993)

itself does not support Euheteroptera but forms a clade consisting of (Gerromorpha + (Dipsocoromorpha + Enicocephalomorpha)), based on the 1-segmented tarsi in the 1st instar nymphs of these taxa (see corrected version of fig. 3). Apomorphic characters shared among Panheteroptera in the morphological analysis are: the absence of arolia in adults (character #21), the differentiation of the fore wing into corium (leathery part) and membrane (character #22), and the interlocking mechanism linking the hemelytra and the body known as ‘Druckknopf’ (character #24) (but see WEIRAUCH & CASSIS 2009 for an alternative interpretation on the evolution of this feature).

In two morphological studies focused on male genital features it was also attempted to shed light on the relative positions of higher-level heteropteran taxa. A “unique position” was assigned to Enicocephalidae based on an unusual feature of the testes (KUMAR 1964). However, it was pointed out in the same study that testes with a single follicle have likely evolved several times independently within different heteropteran families. Moreover, the interpretations were based on a single character system without a sound phylogenetic concept. Based on characters of the male genitalia YANG (2002) suggested Dipsocoromorpha, Gerromorpha and Nepomorpha together to be monophyletic and placed this assemblage as the sister group to Coleorrhyncha (!) + Enicocephalomorpha + (Leptopodomorpha + Cimicomorpha + Pentatomomorpha). Similar to KUMAR (1964), the phylogenetic approach in this study was problematic and character sampling insufficient.

YOSHIZAWA & SAIGUSA (2001) reported a primitive condition of the forewing base structure of Enicocephalidae likely supporting the basal split of Enicocephalomorpha from the rest of Heteroptera.

Similar to the results of WHEELER et al. (1993), Enicocephalomorpha were placed as the most basal branch in the molecular study of XIE et al. (2008). In contrast, Nepomorpha and Leptopodomorpha were placed as the second and third branches, respectively, with (Gerromorpha + Dipsocoromorpha) and (Pentatomomorpha + Cimicomorpha) as sister groups. A basal position of Enicocephalomorpha is also supported by the analysis of 13 protein-coding genes from mitochondrial genomes (Li et al. 2012a). The drawback of this study is the absence of Dipsocoromorpha in the taxon-sampling and the polyphyly of Cimicomorpha.

The hypotheses proposed by SCHUH (1979) and WHEELER et al. (1993), which place Enicocephalomorpha, Dipsocoromorpha and Gerromorpha as basal lineages, are in conflict with several alternative scenarios. Based on morphological data, MAHNER (1993) tentatively suggested “Cryptocerata” (Nepomorpha) as the sister group to the remaining Heteroptera. However, he explicitly pointed out the uncertain position of Enicocephalomorpha and Dipsocoromorpha in this hypothesis, due to the lack of crucial character data. SHCHERBAKOV & POPOV (2002) analyzed 50 morphological characters and like MAHNER (1993) suggested that Nepomorpha may have to be considered as the first branch within Heteroptera. In the

phylogeny of SHCHERBAKOV & POPOV (2002) Enicocephaloidea is placed in the Dipsocoromorpha, which form a clade with Leptopodoidea and Gerromorpha. The most recent and comprehensive multiple gene analysis (18S rDNA, 28S rDNA, 16S rDNA and COI) of Heteroptera was carried out by LI et al. (2012b) using different analytical approaches. Nepomorpha was unambiguously placed as the most basal branch. However, the arrangement of the remaining groups varied very strongly, with Cimicomorpha + Pentatomomorpha being recovered as the only stable sister group relationship among the infraorders (see also WHEELER et al. 1993; XIE et al. 2003; WEIRAUCH & SCHUH 2011). Phylogenetic hypotheses on relationships among the heteropteran infraorders except Cimicomorpha and Pentatomomorpha must therefore be considered tentative at best.

Phylogenetic reconstructions for Heteroptera are clearly impeded by sparse and scattered morphological data. Comprehensive data on the internal cephalic morphology of Enicocephalomorpha and Dipsocoromorpha are currently unavailable (e.g. tentorium, musculature, nervous system) and those on members of the Gerromorpha are very limited. The need for more detailed investigations of head morphology, among other morphological character complexes, is underlined by an erroneous placement of Enicocephalomorpha close to Reduviidae (REUTER 1910; USINGER 1932, 1945; CHINA & MILLER 1959; JORDAN 1972) that was based mostly on superficial similarities of external head structures (SCHUH 1986).

Even though the monophyly of Enicocephalomorpha has not been tested in a phylogenetic framework (see e.g., WEIRAUCH & SCHUH 2011), the group is likely of single origin judging from the uniquely modified head shape, raptorial legs, and distinctive wing venation. Relationships within the group have not been investigated using phylogenetic procedures. The situation is more critical in Dipsocoromorpha, which have long been suspected to be non-monophyletic (WEIRAUCH & SCHUH 2011), although a morphological or combined analysis of the group is lacking as well. However, the first cladistic analysis of Dipsocoromorpha, based on a molecular dataset of 87 Hemiptera including 35 Ceratocombidae, Dipsocoridae, and Schizopteridae, found high support for the monophyly of the entire group and also for the 3 families included in the analysis (WEIRAUCH & ŠTYS in press).

In addition to the striking lack of anatomical data for both Dipsocoromorpha and Enicocephalomorpha, the biology and ecology of Dipsocoromorpha is poorly known.

Enicocephalomorpha (“Henicocephalidae”, Stål, 1860 in USINGER 1932) comprises the two families Enicocephalidae (“Henicocephalinae” in USINGER 1932; 405 species) and Aenictopecheidae (“Aenictopechinae” in USINGER 1932; 20 species) (e.g., CARVER et al. 1991; ŠTYS 1995a, 2008; HENRY 2009). They are characterized by a bilobed head (“unique-headed bugs”) (e.g., KRITSKY 1977) and completely membranous wings with a distinct radius, media and cubitus reaching the posterior margin (e.g., USINGER & WYGODZINSKY 1960; JORDAN 1972; SCHUH & SLATER 1995). The size of the elongated, of-

ten brownish bugs ranges between 2 and 15 mm (ŠTYS 1995a; BANAR 2008; ŠTYS & BANAR 2008). Micropterous and apterous forms are characterized by the loss of ocelli, reduction of eye size and modification of the pronotum (WYGODZINSKY & SCHMIDT 1991). Enicocephalomorpha are predators of different arthropods or polyphagous (e.g., WYGODZINSKY & SCHMIDT 1991). Some species are likely associated with ants (‘myrmecophily’) as different life stages were found in ant nests (summarized in WYGODZINSKY & SCHMIDT 1991 and ŠTYS et al. 2010), but do not necessarily feed on their hosts (SCHUH & SLATER 1995). The area of distribution comprises the southern Nearctic and the Neotropics, the Afrotropical region including Madagascar, the Middle East, the Oriental and Australian regions including New Zealand and the southwestern Pacific (ŠTYS 1995a, 2008).

Dipsocoromorpha comprises the five families Ceratocombidae (52 species), Stemmocryptidae (1 species), Dipsocoridae (51 species), Hypsipterygidae (4 species), and Schizopteridae (229 Species) (HENRY 2009). The dipsocoromorph bugs are characterized by their miniaturization and contain some of the smallest heteropterans (0.5–4 mm) (ŠTYS 1995b). The body is much more compact than in Enicocephalomorpha and the appearance of some taxa is similar to that of beetles (ŠTYS 1995e). A characteristic feature, even though not exclusive to the minute litter bugs, is the long setation on the antennal flagellum in many species (except Stemmocryptidae) (JORDAN 1972; ŠTYS 1995b). Other head structures are quite variable (e.g., presence or absence of ocelli, number and length of labial segments) (SCHUH & ŠTYS 1991; ŠTYS 1995e). Most species are assumed to be predators of small arthropods (CARVER et al. 1991; ŠTYS 1995c,d), but members of some genera of Ceratocombidae have been suggested to feed on molds (ŠTYS 1995c). Hypsipterygidae and Stemmocryptidae are restricted to the Oriental regions, but Ceratocombidae, Dipsocoridae, and Schizopteridae have worldwide distributions, typically with highest diversity in tropical areas (e.g., EMSLEY 1969; CARVER et al. 1991; ŠTYS 1995b). Similar to Enicocephalomorpha, their habitats are rather cryptic and include leaf litter and gravel along river banks, and they also occur in nests of ants (CARVER et al. 1991). Species of Schizopteridae are in addition collected by screen-sweeping vegetation or canopy fogging (C. Weirauch pers. obs.), indicating that some taxa are vegetation dwelling. Early fossils of Dipsocoromorpha are known from the Triassic/Jurassic boundary (SHERBAKOV & POPOV 2002) and the Lower Cretaceous (Schizopteridae) (AZAR & NEL 2010).

In contrast to the former groups, Gerromorpha are very polymorphic and will not be treated here in detail. Instead we refer to ANDERSEN’S (1982) comprehensive compilation on this infraorder. Gerromorpha are either elongate and slender (up to 36 mm in Gerridae) or small and stout (ca. 1 mm in Veliidae) (SCHUH & SLATER 1995). Gerromorph bugs are either polyphagous or predators of other arthropods (CARVER et al. 1991; SCHUH & SLATER 1995). The fossil record of Gerromorpha goes back to the Triassic (DAMGAARD 2008).

In addition to comprehensive molecular data, morphological studies documenting a broad range of character systems and features are necessary for the reconstruction of a well corroborated phylogeny that allows evolutionary interpretations. This is in particular true for Heteroptera, where current phylogenetic hypotheses are unstable and in clear need of additional character data. The main aim of this study is therefore to provide a detailed documentation of the head morphology (including musculature, tentorium, cephalic nervous system and alimentary tract) for representatives of the potentially basal heteropteran lineages Enicocephalomorpha, Dipsocoromorpha and Gerromorpha. This study will close a major gap in the documentation of head structures across Heteroptera (see e.g., PARSONS 1960a, 1962 for studies on Nepomorpha and Leptopodomorpha). In a second step, characters derived from head structures are phylogenetically explored and analyzed using different approaches, with focus on the basal branching pattern in Heteroptera.

2. Material and methods

2.1. Material

The following specimens were examined:

Cryptostemma waltli Fieber, 1860 (Dipsocoromorpha: Dipsocoridae), Germany: Mindelsee (Lake Constance), in pitfall traps on a fallow, 24.x.1989, leg. Kiechle, det. R. Heckmann (same specimens as in HECKMANN & RIEGER 2001), two specimens.

Gerris sp. (Gerromorpha: Gerridae), Germany: Jena, 11°35'07"E 50°54'23"N, vii.2012, leg. et det. R. Spangenberg, one specimen.

Systelloderes sp. (Enicocephalomorpha: Enicocephalidae), Peru: Cuzco: Wayqecha Research Center, 2821 m, 13°10'22"S 71°35'32"W, 05.xii.2011, leg. et det. C. Weirauch, P11L57 sweep, two specimens (same as in SPANGENBERG et al. 2013).

Cryptostemma waltli was killed in formaldehyde and afterwards stored in 70% ethanol. *Gerris* sp. and *Systelloderes* were fixed and preserved in 70% (*Gerris*) and 95% ethanol (*Systelloderes*). In the following all species listed here will be referred to by the generic name only.

2.2. Scanning electron microscopy

Scanning electron (SEM) micrographs of *Systelloderes* and *Cryptostemma* were taken with a Philips XL 30 ESEM (FEI Company, Oregon, USA) and Scandium 5.0 Software (Soft Imaging System GmbH, Münster, Germany). They were completely dehydrated with ethanol (100%) over several stages. Subsequently, the specimens were dried using HMDS (hexamethyldisilazane) (for details see BROWN 1993) and sputter-coated with gold (Em-

iTech K500, Quorum Technologies, West Sussex, UK). A rotatable specimen holder was used to mount the sample (see POHL 2010).

2.3. Cross-section series and 3D-reconstruction

One specimen each of *Cryptostemma*, *Gerris* and *Systelloderes* was embedded in Araldite® (Huntsman Advanced Materials, Bergkamen, Germany) for semi-thin cross sectioning (1 µm; *Cryptostemma*, *Systelloderes*) or longitudinal sectioning (1 µm; *Gerris*) with a glass knife on a microtome HM 360 (Microm, Walldorf, Germany). The sections were stained with toluidin-blue. Images of sections for 3D-reconstruction of *Cryptostemma* and *Systelloderes* were taken with a Zeiss Axioplan (Zeiss, Göttingen, Germany), the AnalySIS® documentation system (Soft Imaging System GmbH, Münster, Germany) and a pixelink CCD-camera (PixeLINK, Ottawa, Canada). Figures were processed in Adobe® Photoshop® CS2 Version 9.0 (Adobe Systems Incorporated San Jose, California, USA) and Adobe® Illustrator® CS2 12.0.0 (Adobe Systems Incorporated, San Jose, California, USA). Alignment and three-dimensional reconstructions were done with Mercury Amira® 4.1.2 (Visage Imaging GmbH, Berlin, Germany) and surfaces were smoothed with Autodesk Maya® 7.0 (Autodesk GmbH, Munich, Germany).

2.4. Terminology

The terms dorsal, ventral, anterior and posterior consistently refer to the longitudinal body axis (e.g., vertex dorsal, labium ventral), the mouthparts being considered as extending anteriorly from the head capsule (prognathous condition). Muscles are continuously numbered in order of appearance and follow the terminology established in SPANGENBERG et al. (2013). The definition of ridges, sutures and tentorium follows WIPFLER et al. (2011). A suture is interpreted as ecdysial cleavage line whereas a ridge is a cuticular strengthening. In some cases an adaptation of this terminology is necessary to facilitate the morphological comparison of different borders throughout the infraorders and with other studies (i.a. "mandibular sulcus", see 3.1. Head).

2.5. Cladistic analysis

The analysis comprises 61 characters of the head of 16 representatives of Heteroptera and two outgroup taxa. Winclada 1.00.08 (NIXON 2002) was used for compiling the matrix and NONA (Ratchet, search settings: 1000 replicates) (GOLOBOFF 1999) and TNT (GOLOBOFF et al. 2008) (Settings Memory: General Ram 200 Mbytes,

Max. trees 99999; Analyze Traditional Search, random seed 999999) for calculating minimum length trees. Only unambiguous character transformations were evaluated. Branch support values (BREMER 1994) were calculated with the “Bremer Support” function implemented in TNT (calculate support with TBR, collapse nodes with support below 0, retain trees suboptimal by 30 steps). Characters were coded as non-additive and of equal weight. For additional character evaluations and character mapping three alternative topologies on earlier hypotheses (WHEELER et al. 1993; MAHNER 1993; SHCHERBAKOV & POPOV 2002; LI et al. 2012; XIE et al. 2008) were enforced with Winclada (“move branch mode”). The “collapse node mode” was used for collapsing relationships within the infraorders.

3. Results

3.1. *Systelloderes* (Enicocephalomorpha)

The head structures are treated starting with the head capsule, followed by the appendages, the digestive tract including salivary complex, and finally the elements of the cephalic nervous system. The muscles belonging to these structures are treated in the corresponding subsections.

Head capsule

The elongated, prognathous head is very distinctly divided into a cylindrical anterior part, a large globular middle part and a smaller globular occipital region (Fig. 1). The three cephalic portions are separated from each other by constrictions extending across the dorsal and lateral parts of the head. The anterior and middle portions are densely covered with long setae. Minute setae are also present but restricted to the ventro-lateral areas. Pairs of cephalic trichobothria are not recognizable.

The anterior part is formed by the flattened frons (fr), which is located dorsally between the globular compound eyes (ce) (Fig. 1A,B). It is separated from the clypeus by the epistomal ridge (epr) (Fig. 2B). However, the internal strengthening is less distinct. The compound eyes are slightly located ventrad. They are enclosed by a weakly developed circumocular ridge (cor) and bear two setae in the posterior part (Fig. 1B). The ventro-lateral region of the anterior part of the head capsule is formed by the genae (ga). They expand upward in front of the maxillary plates to form a collar, and their anterior margin articulates with the basal margin of the labium (Fig. 1B). Bucculae (“flanges of gena, on each side of basal portion of labium” [SCHUH & SLATER 1995]) are not developed. The bases of the antennae are located laterally and anterad of the compound eyes. Mandibular and maxillary plates are present on the antero-dorsal side of the anterior head por-

tion between the bases of the antennae. The small triangular and glabrous mandibular plates or lora (lor) originate at the fronto-clypeal border region (cly). Along their posterior margins they are separated from the remainder of the head capsule by the genal suture (gs) (see ANDERSEN 1982). In the stricter sense this is no ecdysial cleavage line (see 2.4.). However, we apply this term for comparison with the detailed study of ANDERSEN (1982). Mesally the lora extend beneath the clypeus along the clypeolateral cleft (clc) (Figs. 1B, 2B). The plates are fused with each other medially beneath the clypeus (Fig. 8D) and with the head capsule on their ventral side caudally. The lora form the dorsal guiding device for the feeding stylets (Figs. 3, 8D). The rectangular, sclerotised maxillary plates (mxpl) bear three long setae on their anterior part and originate anterad the apex of the mandibular plates. They are separated from the latter by the mandibular sulcus (msu) (see SINGH 1971; “lorogenal cleft” of PARSONS 1968) and from the collar-like part of the genae by the ventral cleft (vc) (Figs. 1B, 2B). The maxillary plates are divided into two bean-shaped subunits which are connected basally. The outer ones enclose the ventrolateral margins of the clypeus (Fig. 8C). The inner subunits are not visible externally (Fig. 3A). They lie below the clypeus and both structures together form the ventral guiding device for the feeding stylets (Fig. 3A). Subgena, subgenal ridges and the frontal and coronal (= epicranial) sutures are not distinguishable.

The middle cephalic subunit is the broadest and highest part of the head capsule and bears a median longitudinal incision. It is mainly formed by the vertex (vx) dorso-laterally (and likely the occiput posteriorly) (Fig. 1A). The paired ocelli (oc) in the postero-dorsal region are separated by the longitudinal incision (Fig. 1A). The ventral closure of the head capsule is not subdivided by any ridges or sutures and tentatively referred to as “gular region” (gu) (Fig. 1B,C).

The postoccipital region (poc) is separated from the middle cephalic region by a weakly developed ridge (pocr) (Fig. 1A). This region of the head capsule is partly retracted into the prothorax (pt) and both structures together form a ball-and-socket joint (Figs. 1B, 3A). The thickness of the lateral sides of the postoccipital region is partly increased (stout paired cuticular condyles, indicated by arrows in Figs. 3 and 9L). The dorsal side is formed by a sclerotised, but thin, lip-like apodeme (Fig. 3A). The diameter of the foramen occipitale is slightly smaller than that of the postoccipital region. The latter merges continuously with the cervix (cv) (Figs. 3A, 9L,M).

Musculature. (M1–M5b). M1 (Figs. 3B, 9M,N): O (= origin) – laterally on the pronotum; I (= insertion) – laterally on the dorsal apodeme of the postocciput; F (= function) – levator and retractor of the head (simultaneous contraction) or rotator. M1a (muscles with a small letter are treated as a separate unit) (Fig. 3B): minute transverse muscle ventrad the anterior region of the dorsal apodeme. M2 (Figs. 3B, 9M,N): O – mesonotum; I – dorsolaterally on the dorsal apodeme; F – levator of the

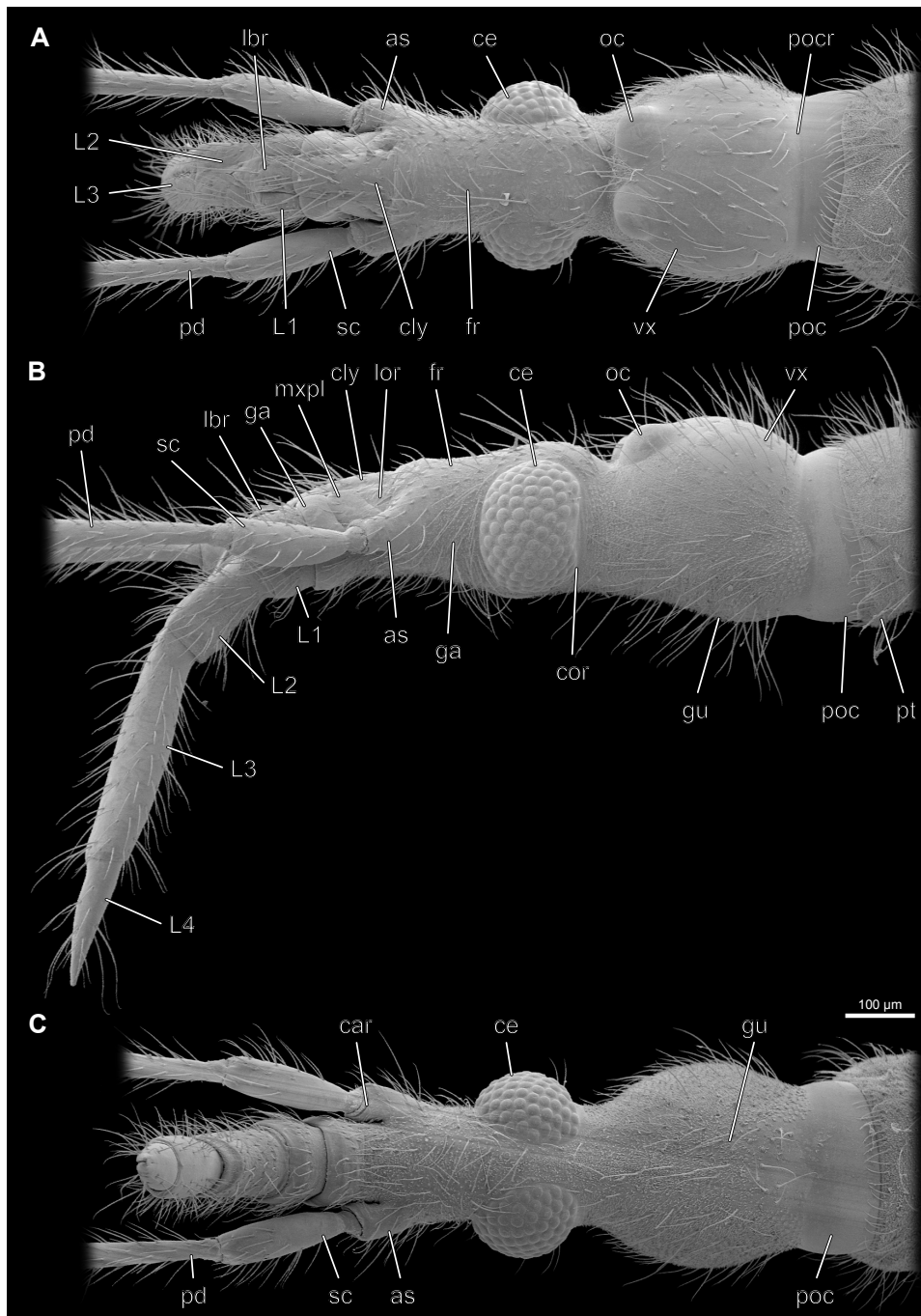


Fig. 1. *Systelloderes* sp.: head and thorax, basi- and distiflagellum omitted, Scanning Electron Micrograph (SEM). **A:** dorsal view; **B:** lateral view; **C:** ventral view. as, antennal socket; car, circumantennal ridge; ce, compound eye; cly, clypeus; cor, circumocular ridge; fr, frons; ga, genal area; gu, gular region; L1–L4, labial segment 1–4; lbr, labrum; lor, lorum/mandibular plate; mxpl, maxillary plate; oc, ocellus; pd, pedicellus; poc, postoccipital region; pocr, postoccipital ridge; pt, prothorax; sc, scapus; vx, vertex.

head. M2a (Figs. 3B, 9M): O – laterally on the pronotum, anterad M1; I – dorsomedially on the dorsal apodeme; F – levator of the head. M3 (Figs. 3A, 9M,N): O – mesal region of the pronotum; I – ventrolaterally on the postocciput; F – depressor of the head. M4 absent. M5 (Figs. 3B, 9M,N): O – anterior side of the profurcal arm; I – ventrolaterally on the cervical membrane, posterad the ventral region of the foramen occipitale; F – depressor and retractor of the head. M5a absent. M5b (Figs. 3B, 9M,N): O – anterior side of the profurcal arm, laterad

of M5; I – ventrolaterally on the cervical membrane and laterad M5, posterad the ventral region of the foramen occipitale; F – depressor and retractor of the head.

Tentorium

The tentorium is completely reduced. Anterior and posterior tentorial pits are not developed. Sclerotised elements not belonging to the tentorium but lying within the head cap-

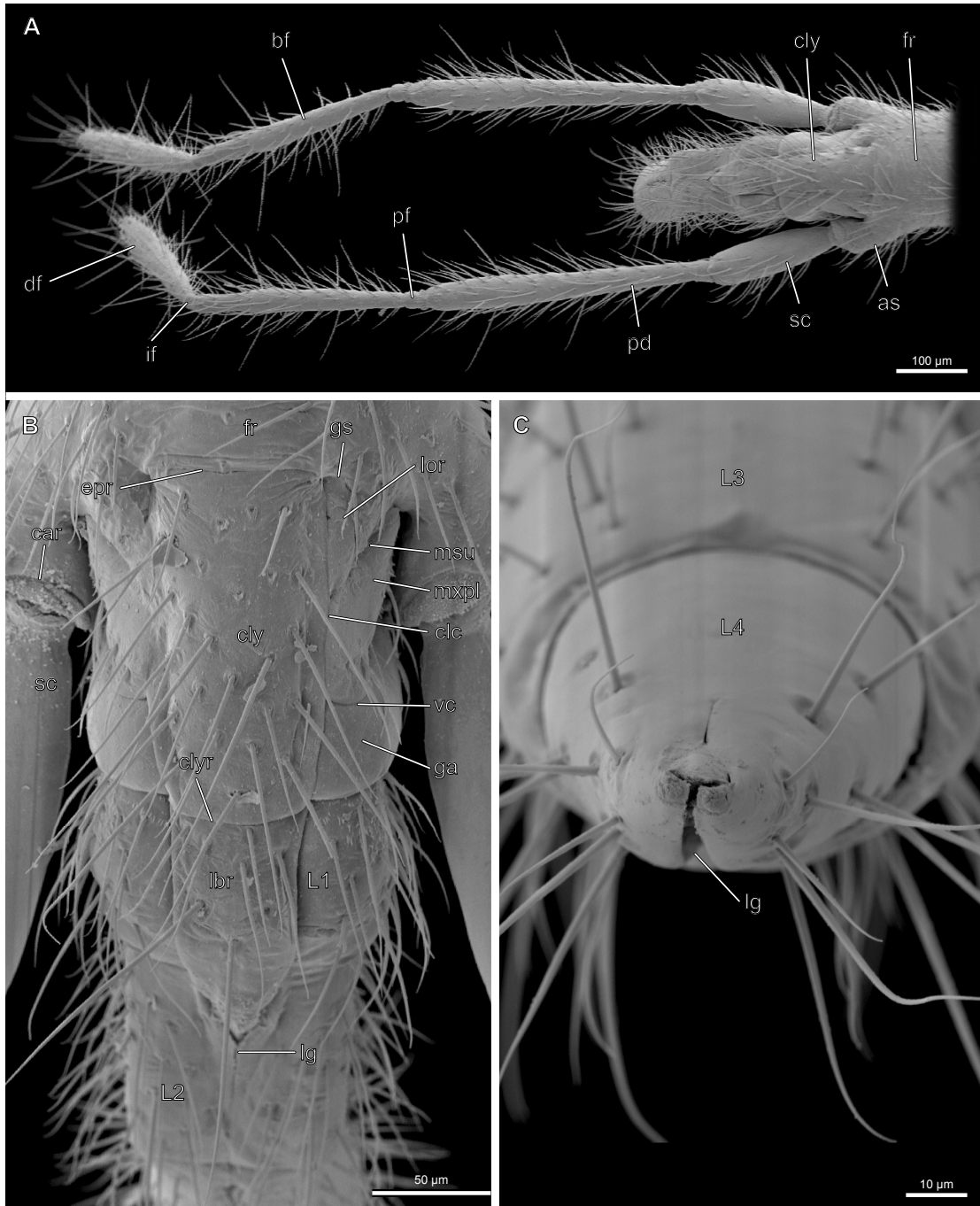


Fig. 2. *Systelloderes* sp.: head, SEM. **A:** dorsal view; **B:** dorsal view, enlarged detail of Fig. 2A; **C:** tip of labium, enlarged detail of Fig. 1C. as, antennal socket; bf, basiflagellum; car, circumantennal ridge; clc, clypeolateral cleft; cly, clypeus; clyr, clypeo-labral ridge; df, distiflagellum; epr, epistomal ridge; fr, frons; ga, genal area; gs, genal suture; if, intraflagelloid; L1–L4, labial segment 1–4; lbr, labrum; lg, labial groove; lor, lorum/mandibular plate; msu, mandibular sulcus; mxpl, maxillary plate; pd, pedicellus; pf, preflagelloid; sc, scapus; vc, ventral cleft.

sule are the hypopharynx, the hypopharyngeal wings, the piston of the salivary pump and the mandibular and maxillary lever, which are treated in the following chapters.

Clypeus and labrum

The rectangular and slightly convex clypeus (cly) is not divided into an anteclypeus, paraclypeus and postclypeus. Its dorsal side is densely covered with long setae (Figs.

1B, 2B). A longitudinal rim functioning as a guiding device for the stylets is present on the ventral side (indicated by an arrow in Fig. 8B). The ventrolateral area of the middle region is interlocked longitudinally with the parts of the gena and of the mandibular plates that lie beneath the clypeus, for further mechanical support during feeding (Fig. 8D).

The tongue-shaped labrum (lbr) originates along the distal margin of the clypeus (Fig. 1A,B). It is separated from the clypeus by a distinct clypeo-labral ridge (clyr)

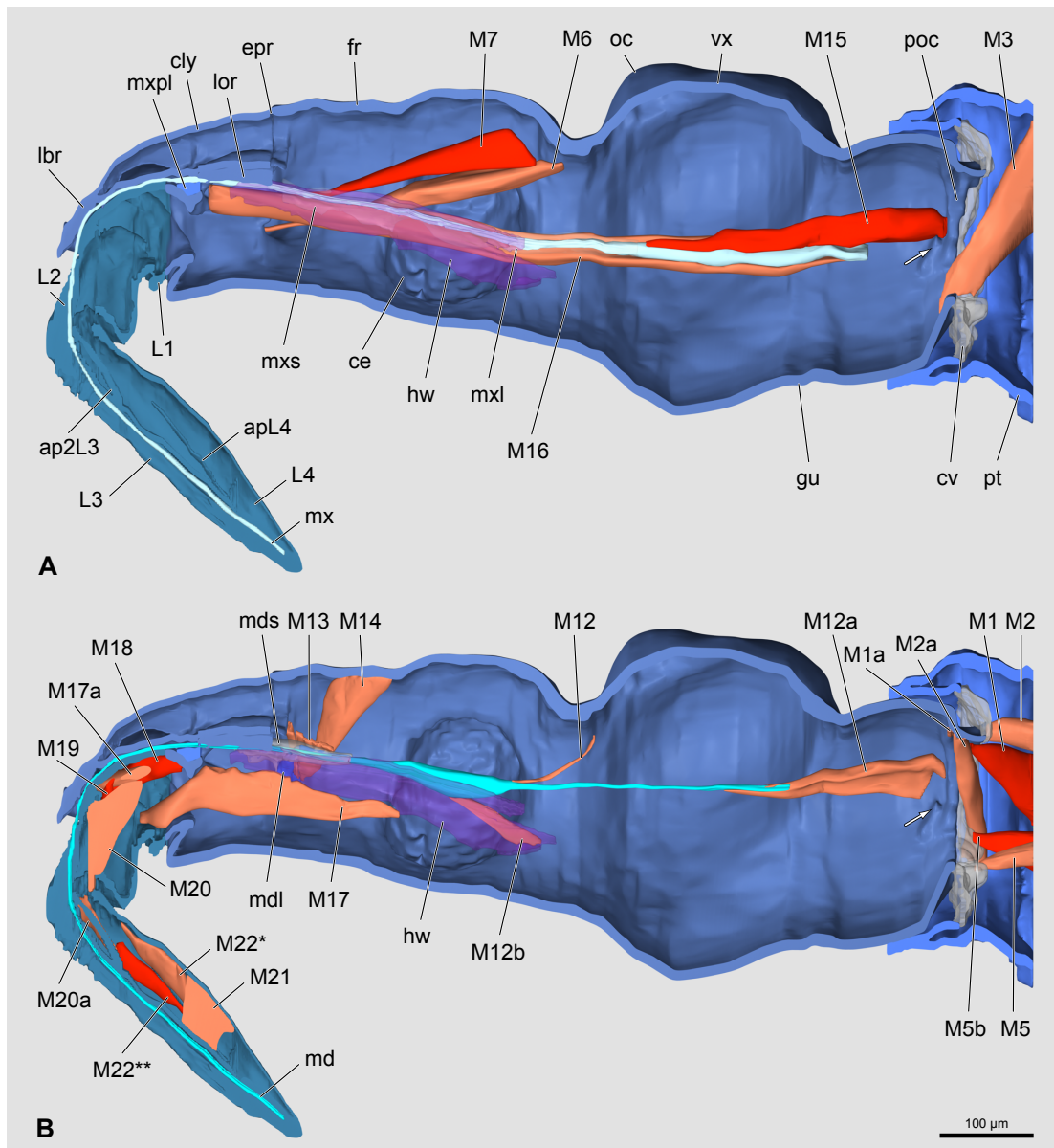


Fig. 3. *Systelloderes* sp.: head and thorax, 3D-reconstruction, sagittal section, different muscles and feeding stylets shown (blue: sclerotization, grey: membrane, red: musculature). ap2L3, unpaired bar-shaped apodeme of the 3rd labial segment; apL4, apodeme of 4th labial segment; ce, compound eye; cly, clypeus; cv, cervical membrane; epr, epistomal ridge; fr, frons; gu, gular region; hw, hypopharyngeal wing (semitransparent); L1–L4, labial segment 1–4; lbr, labrum; lor, lorum/mandibular plate; M, muscle with appropriate number (number of muscle corresponds to number in text, Figs. 4–9, Tables 1, 2); md, mandible; mdl, mandibular lever; mds, mandibular sac; mx, maxilla; mxl, maxillary lever; mxpl, maxillary plate; mxs, maxillary sac (semitransparent); oc, ocellus; poc, postoccipital region; pt, prothorax; vx, vertex. Arrow in (B) indicates each partly increased thickness of lateral sides of postoccipital region (see also Fig. 9L).

(Fig. 2B). The dorsal side is densely covered with setae posteriorly while the clypeal longitudinal guiding rim is continued on its ventral side (Fig. 3A). The labrum covers the first labial segment and the base of the second one (Fig. 2B).

Musculature. No muscles are associated with the clypeus and the labrum. M10 and M11 absent.

Antennae

The four-segmented antennae are inserted on a promi-

nent antennal socket (as) anterad the compound eyes and laterad the mandibular and maxillary plates (Figs. 1, 2A). The circumantennal ridge is distinct (car) (Figs. 1C, 2B). An antennifer is absent. The scapus (sc) is cylindrical, densely covered with setae on its lateral side and half as long as the pedicellus (Fig. 2A). The histological section in the plane of the base of the scapus shows two bean-shaped sclerites embedded in the membrane, the “scapus sclerites” (ss) (Figs. 7, 8D). The pedicellus (pd) is more narrow and all sides are covered with setae (Fig. 2A). Its base is connected with membranes to a minute oval sclerite laterally (pp, Fig. 7). This likely

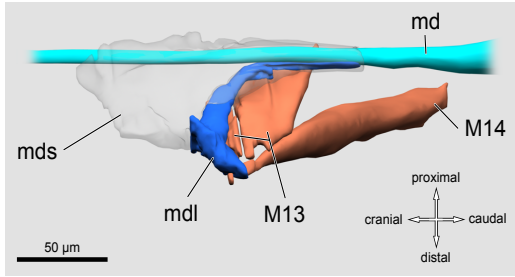


Fig. 4. *Systelloderes* sp.: detail of mandible connected with mandibular lever, 3D-reconstruction (blue: sclerotization, red: musculature). M, muscle with appropriate number (number of muscle corresponds to number in text, Figs. 3, 5–9, Table 1); md, mandible; mdl, mandibular lever; mds, mandibular sac.

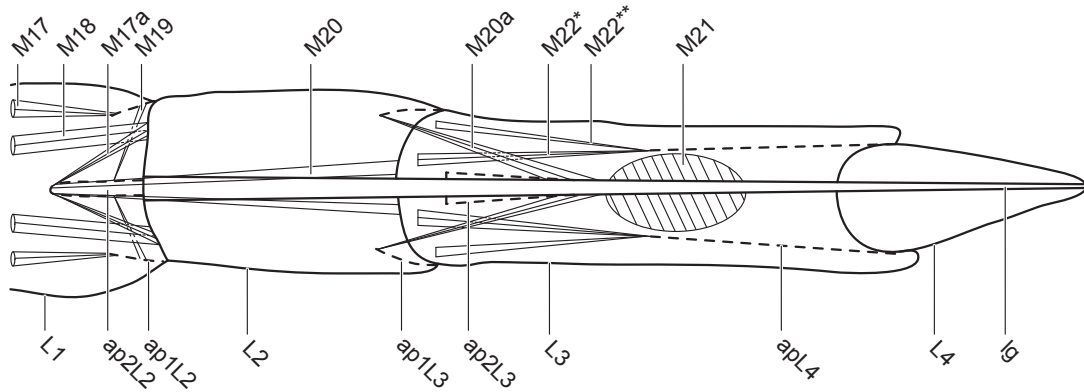


Fig. 5. *Systelloderes* sp.: labium schematic (transparent) and elongated, dorsal view. ap1L2, apodeme of 2nd labial segment; ap2L2; unpaired apodeme of 2nd labial segment; ap1L3, apodeme of 3rd labial segment; ap2L3, unpaired apodeme of 3rd labial segment; apL4, apodeme of 4th labial segment; L1–L4, labial segments 1–4; lg, labial groove; M, muscle with appropriate number (number of muscle corresponds to number in text, Figs. 3, 4, 6–9, Table 1).

represents the “prepedicellite” of ZRZAVÝ (1990). The flagellomere comprises the “basiflagellum” or “basiflagellite” (bf) and “distiflagellum” or “distiflagellite” (df) (see ZRZAVÝ 1990) (Fig. 2A). They are similar in shape, length and setation to the pedicellus. A separate globular and glabrous sclerite is present between the pedicellus and basiflagellum, and between the basiflagellum and distiflagellum, respectively. They likely represent the “preflagelloid Type II” (pf) and “intraflagelloid Type I” (if) of ZRZAVÝ (1990: “hardly sclerotised, thick-walled cylinder with the diameter approximately equal to the height”) (Fig. 2A).

Musculature. Extrinsic and intrinsic antennal muscles (M6–M9). M6 (Figs. 3A, 7, 9I): O – roof of the head capsule, border region of the anterior and middle part; I – posterad the ventral base of the scapus; F – depressor of the antenna. M7 (Figs. 3A, 7, 9I): O – roof of the head capsule, anterad O of M6; I – posterad the dorsal base of the scapus; F – levator of the antenna. M8 (Figs. 7, 8B): O – proximal base of the scapus; I – proximal base of the pedicellus; F – extensor of the pedicellus. M9 (Figs. 7, 8B): O – distal base of the scapus; I – distal base of the pedicellus; F – flexor of the pedicellus.

Mandible

The mandibles (md) are a pair of symmetrical, long and slender stylets. Their bases are deeply sunk into the head

capsule. Two thirds of their entire length is situated in the head capsule where they reach the posterior margin of the middle cephalic part (Fig. 3B). The proximal halves follow the longitudinal body axis while the distal parts are strongly bent ventrocaudad in resting position (Fig. 3B). The distal parts are crescent-shaped in cross section, with protruding inner edges. They partly enclose the maxillae (Fig. 10). The curved part starts at the level of the first labial segment (L1) (Fig. 3B). The mandibular part located mesad the compound eyes forms a hollow widened tube which opens posterad (Fig. 3B, 8G). The lumen reaches into the apical part (Fig. 10). The proximal opening of the mandibular base is transformed into a long and slender cuticular tendon dorsally (Figs. 3B, 9J).

The mandibles are connected with a curved, acutely triangular, sclerotised mandibular lever (mdl) (type III of RIEGER 1976). It is located at a level posterad the antennal socket. The mandibular lever tapers caudally and is transformed into a longitudinal sclerotised stripe anterad the widening (Fig. 4). Only this stripe-part is connected with the mandible directly. The membranous mandibular sac (mds) is attached to the proximal end of the lorum. It partly surrounds the proximal region of the lever and the stylet in the region of the antennal socket (Figs. 3B, 4 and 8E). Mandibular glands are absent.

Musculature. Retractor and promoters of the mandibular stylet (M12–M14). M12 (Fig. 3B): very thin muscle, O – dorsally on the head capsule, on the constriction between the anterior and middle part; I – posterad the widen-

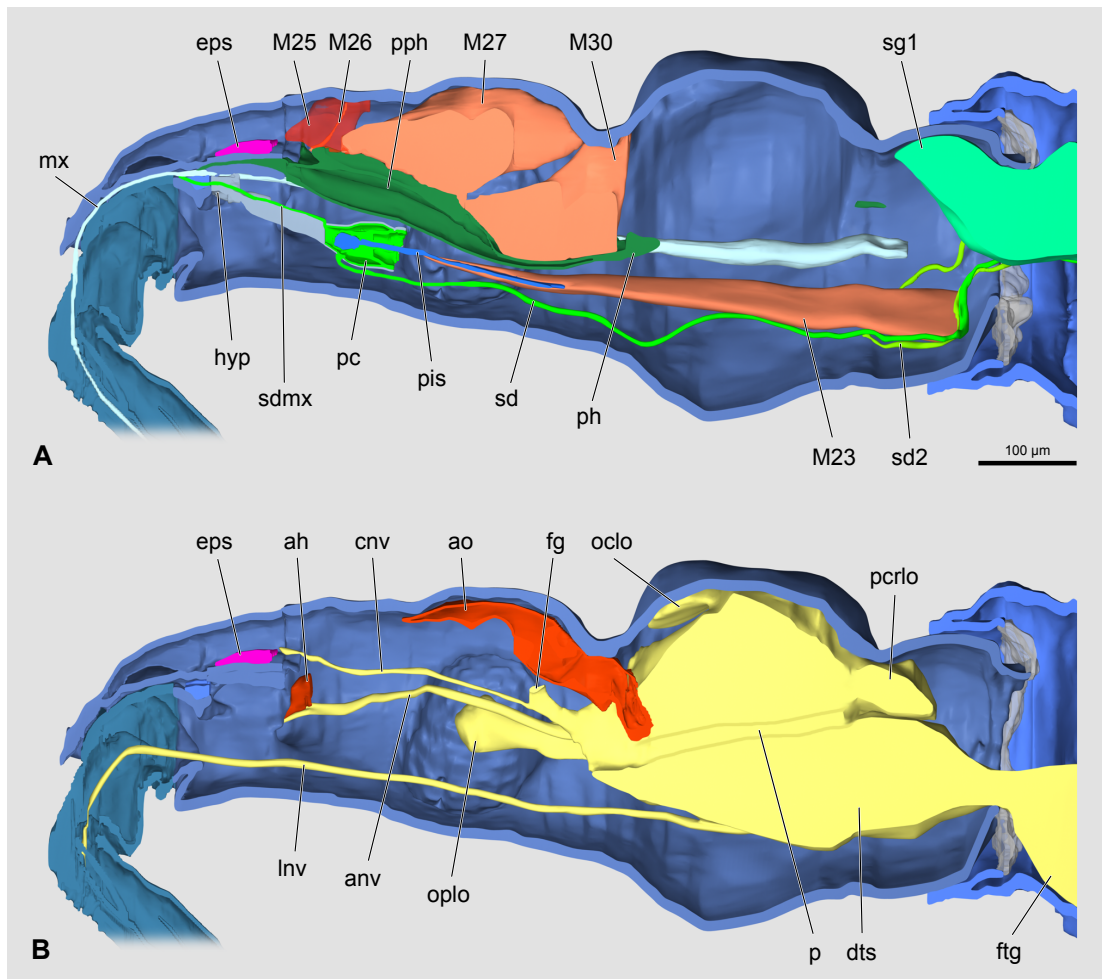


Fig. 6. *Systelloderes* sp.: head and thorax, 3D-reconstruction, sagittal section, different muscles, alimentary system (A) and nervous system (B) shown (blue: sclerotization, dark green: pharynx, light green: salivary complex, red: musculature, yellow: nervous system). ah, antennal heart; anv, antennal nerve; ao, aorta cephalica; cnv, clypeo-labral nerve; dts, deuto-tritocerebrum-subesophageal-complex; eps, epipharyngeal sense organ; fg, frontal ganglion; ftg, first thoracal ganglion; hyp, hypopharynx; Inv, labial nerve; M, muscle with appropriate number (number of muscle corresponds to number in text, Figs. 3–5, 7–9, Table 1) (M25 semitransparent); mx, maxilla; oclo, ocellar lobe; oplo, optic lobe; p, passage through brain for aorta and pharynx; pc, pumping chamber; pcrlo, protocerebral lobe; ph, pharynx; pis, piston; pph, prepharynx; sd, common salivary duct; sd2, accessory duct; sdmx, salivary duct connecting pump chamber with salivary channel of maxillae; sg1, principal duct.

ing of the mandible; F – retractor. M12a (Figs. 3B, 9K,L): O – laterally on the distal postoccipital region, dorsad the strengthening of the postoccipital region; I – bar-shaped region of the mandible; F – retractor. M12b (Figs. 3B, 8H, 9I): two small bundles, attached to M16, O – proximal end of the hypopharyngeal wing; I – ventrally on the widened part of the mandible; F – third retractor. M13 (Figs. 3B, 4, 8E): O – dorsally on the border region of head capsule and clypeus; I – laterally on the mandibular lever; F – protractor. M14 (Figs. 3B, 4, 8E): O – dorsally on the roof of the head capsule, anterad the compound eyes; I – laterally on the mandibular lever; F – protractor.

Maxilla

The maxillae consist mainly of the very elongate lacinae. The palp and galea are absent. The proximal elements

appear indistinguishably fused, without a recognizable detachment of the lacina from the stipes. The lacinae, probably together with the parts corresponding with the cardo and stipes (mx), form a pair of hollow, slender stylets. Two thirds of their entire length is situated within the head capsule. Proximally the maxillae reach the anterior region of the posterior cephalic part (Figs. 3A, 9J). The right maxilla originates more proximally than the left one (Fig. 9K). The distal thirds of the stylets (from the beginning of the base of the mandibular plates) are linked with each other forming a dorsal food channel and a ventral salivary channel, with the mesal regions each forming a curved “E” in cross section, with three sclerotised extensions. The food channel (fc) is about twice as large as the salivary channel (sa) and is formed by both stylets to the same extent. In contrast, the ventral extension of the left maxilla is more prominent and thus encloses a larger part of the salivary channel (Fig. 10). The E-shaped structure

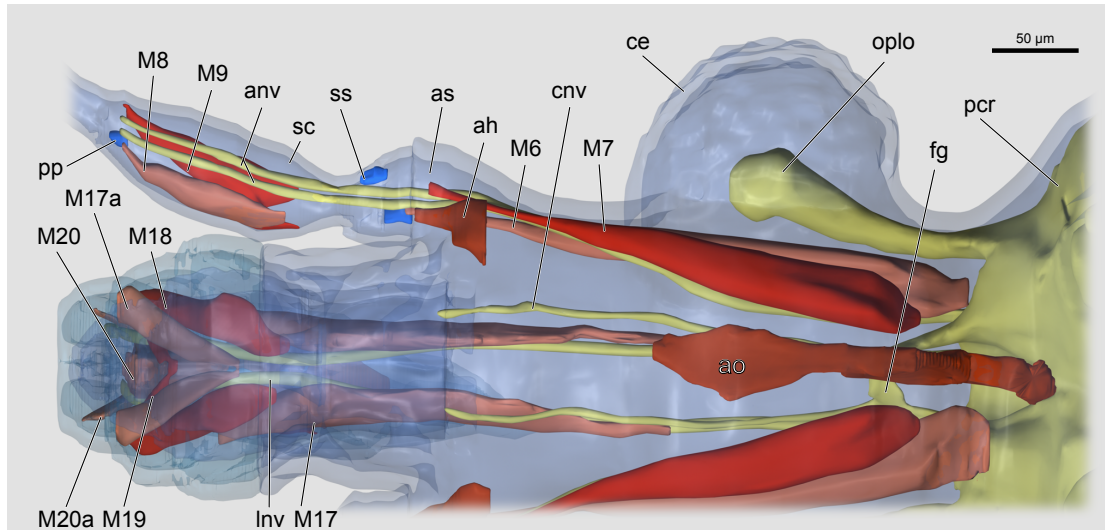


Fig. 7. *Systelloderes* sp.: head (semitransparent), 3D-reconstruction, dorsal view (blue: sclerotization, red: musculature and aorta, yellow: nervous system). ah, antennal heart; anv, antennal nerve; ao, aorta cephalica; as, antennal socket; ce, compound eye; cnv, clypeo-labral nerve; fg, frontal ganglion; Inv, labial nerve; M, muscle with appropriate number (number of muscle corresponds to number in text, Figs. 3–6, 8, 9, Table 1); oplo, optic lobe; pcr, protocerebrum; pp, prepedicellite; sc, scapus; ss, scapus sclerite.

reaches the region posterad the compound eyes (Fig. 9I). The following proximal part of the maxilla is an almost circular widened tube with the opening posterad (Fig. 9J). The membranous maxillary sac (mxs) covers the stylets along the hypopharyngeal wing and maxillary lever (Figs. 3A, 8E). The sac ends proximad the end of the E-shaped region. It is apparently not linked with the head capsule. Maxillary glands are not present.

Musculature. Retractor and promotor of the maxillary stylet (M15, M16). M15 (Figs. 3A, 9J,L): O – laterally on the distal postoccipital region, dorsad the strengthening of the foramen occipitale, ventrad O of M12a; I – dorsally on the maxillary stylet, posterad the E-shaped structure; F – retractor. M16 (Figs. 3A, 9J): one of the largest intrinsic cephalic muscle, O – on the border region of the hypopharynx and maxillary plate; I – ventrolaterally on the proximal circular stylet region; F – promotor.

Labium

The tube-like, four-segmented labium (lab) forms the anterior closure of the head capsule (Fig. 1) and a sheath for the mandibles and the maxillae (Fig. 3). This functional complex is called the “feeding tube” or “suctorial beak”. In its resting position its tip is directed ventrally to ventrocaudally (Figs. 1B, 3). The exposed surface of the labium is covered with long setae (Fig. 1B). The proximal sides of segments three and four are glabrous (Fig. 1C). The labial groove (lg) is situated on the distal side of segments two to four (Figs. 2B,C, 5). The four segments are separated from each other by articulation membranes (Fig. 1C). The basal segment (L1) is the shortest (Fig. 1).

The feeding stylets are placed in a shallow depression on its dorsal side and covered by the clypeus and labrum (Fig. 3.). The second segment (L2) is twice as long as L1. A slender, deep incision on its dorsal side forms transition to the labial groove (Figs. 1B, 2B). Its proximal region is partly retracted into the basal segment. A pair of lateral apodemes originates from its base (ap1L2) and an unpaired bar-shaped apodeme medially from its dorsal edge (ap2L2) (Fig. 5). The third segment (L3) is the longest and twice as long as L2 (Fig. 1B). Its base is partly retracted and bears an apodeme on both sides (ap1L3) (Fig. 5). The floor of the proximal labial groove is strongly sclerotised and forms a bar-shaped apodeme anteriorly (ap2L3) (Figs. 3A, 5). The lateral edges of the groove are interlocked with each other by a groove-and-tongue connection. Two sclerotised extensions (“tongues”) on the left side fit with the corresponding folds (“grooves”) on the right side (indicated by arrows in Figs. 8B–D). The interlocking mechanism is less tight in the basal and distal region of the segment. The cone-shaped apical labial segment (L4) is about as long as L2 (Fig. 1B). Two bar-shaped apodemes (apL4) originate on its base and reach into L3 over half its length (Figs. 3A, 5). Three furrows are present at the apex. A row of sensilla is not recognizable (Fig. 2C). Intercalary sclerites are not present in the labium.

Musculature. Extrinsic and intrinsic labial muscles (M17–M22). M17 (Figs. 3B, 5, 7, 8G): largest extrinsic labial muscle, O – ventrally on the anterior half of the hypopharyngeal wing; I – ventrally on the base of L2; F – extensor of the labium. M17a (Figs. 3B, 5, 7, 8B): O – laterally on the proximal part of the unpaired apodeme ap2L2; I – distal region of L1, dorsad the paired apodeme ap1L2; F – flexor of the labium (simultaneous contraction) or rotator. M18 (Figs. 3B, 5, 7, 8B): O – dorsally on the roof of the anterior part of the head capsule; I – near

¹ The terms distal, proximal, dorsal and ventral refer to the position of the labium as seen in Fig. 1B.

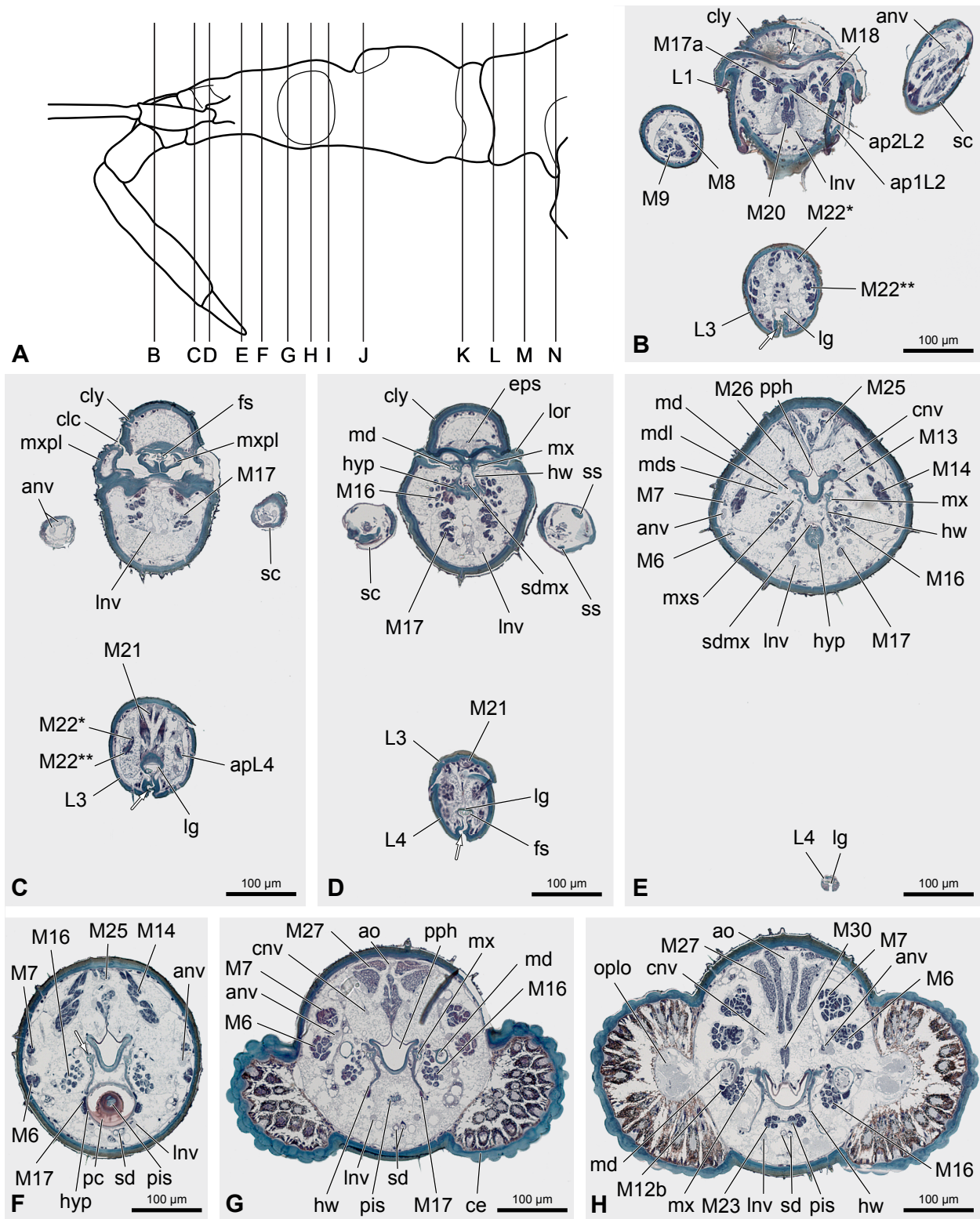


Fig. 8. *Systelloderes* sp.: head and thorax, cross sections. **A:** head and thorax, schematic, lateral view showing planes of section of light micrographs **B–N** (continued in Fig. 9). anv, antennal nerve; ao, aorta cephalica; apL4, apodeme of 4th labial segment; ce, compound eye; clc, clypeoloral cleft; cly, clypeus; cnv, clypeo-labral nerve; eps, epipharyngeal sense organ; fg, frontal ganglion; fs, feeding stylets; hw, hypopharyngeal wing; hyp, hypopharynx; L1–L4, labial segment 1–4; lg, labial groove; Inv, labial nerve; lor, lorum/mandibular plate; M, muscle with appropriate number (number of muscle corresponds to number in text, Figs. 3–7, 9, Table 1); md, mandible; mdl, mandibular lever; mds, mandibular sac; mx, maxilla; mxpl, maxillary plate; mxs, maxillary sac; oplo, optic lobe; pc, pumping chamber; pis, piston; pph, prepharynx; sc, scapus; sd, common salivary duct, sdmx; salivary duct connecting pumpnig chamber with salivary channel of maxillae; ss, scapus sclerite. Upper arrow in (B) indicates longitudinal rim functioning as a guiding device for the stylets (the latter are damaged in this slice); lower arrow in (B–D) indicates interlocking of lateral edges of labial groove. Arrow in (F) indicates linkage of maxillae and hypopharyngeal wing (see also Fig. 8E,G).

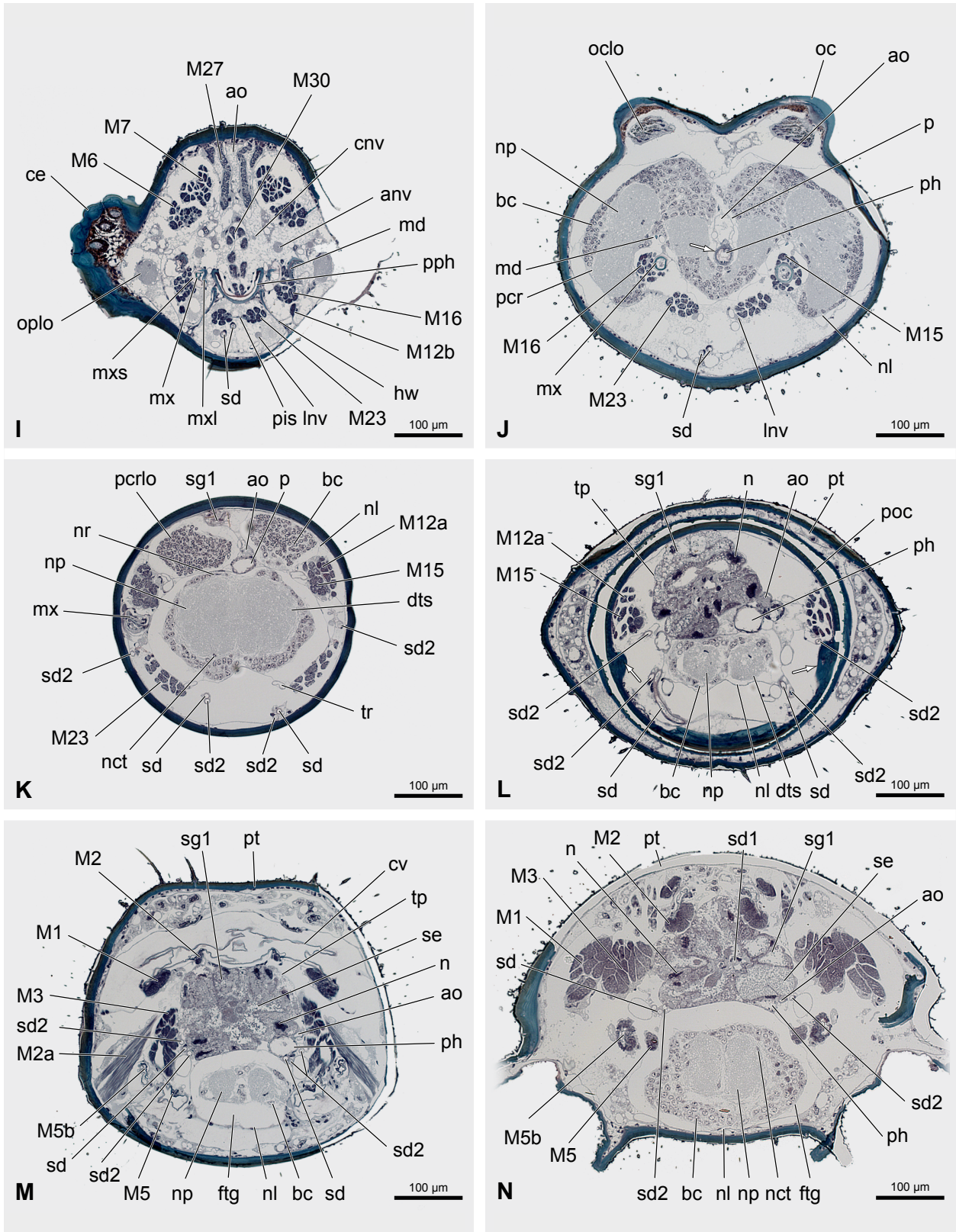


Fig. 9. *Systelloderes* sp.: head and thorax, cross sections, Fig. 8 continued. anv, antennal nerve; ao, aorta cephalica; bc, bark cell; ce, compound eye; cnv, clypeo-labral nerve; dts, deuto-tritocerebrum-subesophageal-complex; ftg, first thoracal ganglion; hw, hypopharyngeal wing; Inv, labial nerve; M, muscle with appropriate number (number of muscle corresponds to number in text, Figs. 3–8, Table 1); md, mandible; mx, maxilla; mxl, maxillary lever; mxs, maxillary sac; n, nucleus; nct, nucleus of connective tissue; nl, neural lamella; np, neuropil; nr, neurilemma; oc, ocellus; oclo, ocellar lobe; oplo, optic lobe; p, passage through the brain for pharynx and aorta; pcr, protocerebrum; ph, pharynx; pis, piston; poc, postoccipital region; pph, prepharynx; pt, prothorax; sd, common salivary duct; sd1, principal duct; sd2, accessory duct; se, secretion granules; sg1, principal gland; tp, tunica propria; tr, trachea. Arrow in (J) indicates ring muscle layer. Arrow in (L) indicates each partly increased thickness of lateral sides of postoccipital region (see also Fig. 3).

the paired apodeme ap1L2, ventrad I of M17; F – flexor of the labium (simultaneous contraction) or rotator. M19 (Figs. 3B, 5, 7): smallest labial muscle, O – laterally on the unpaired apodeme ap2L2; I – paired apodeme ap1L2, ventrad I of M18; F – support of M17 and M18. M20 (Figs. 3B, 5, 7, 8B): largest intrinsic labial muscle, unpaired, O – ventrally on the unpaired apodeme ap2L2 and dorsally on L2; I – dorsally on L3 and its paired apodemes; F – flexion of L3 and L4. M20a (Figs. 3B, 5, 7): O – laterally on the apodemes ap1L3; I – strengthening of the floor of the labial groove in L3; F – pulls the floor of the labial groove upwards, closes the lateral sides of the labial groove (locking mechanism of the feeding stylets). M21 (Figs. 3B, 5, 8C): unpaired, stout muscle, O – dorsal region of L3, posterior part; I – floor of the labial groove in L3; F – pulls the floor of the labial groove upwards and closes the lateral sides of the labial groove (locking mechanism of the feeding stylets) and likely extension of L4 (connection over the labial floor). M22* (Figs. 3B, 5, 8B): first partition of M22, O – dorsal region of L3, anterior part; I – dorsally on the apodemes apL4; F – flexion (simultaneous contraction) or rotator of L4. M22** (Figs. 3B, 5, 8B): second partition of M22, O – laterally on the anterior side of L3; I – ventrally on the apodemes apL4; F – flexion (simultaneous contraction) or rotator of L4.

Hypopharynx, salivary pump and salivary glands

The sclerotised hypopharynx (hyp) is composed of a slender flattened anterior part (“hypopharyngeal lobe” of CRANSTON & SPRAGUE 1961) and a widened area posterad. The anterior part is fused with the head capsule at a level of the base of the maxillary plates, and is partly connected by membranes with the base of the mesal region of the mandibular plate (Figs. 6A, 8D). In this area it forms two protrusions dorsally which enclose the efferent salivary duct (sdmx, see below) (Fig. 8D). The posterior third of the hypopharynx is almost globular and widens to a bowl-shaped structure enclosing the membranous pumping chamber (Figs. 6A, 8E,F).

The plate-like hypopharyngeal wing (hw) arises at the anterior fifth of the hypopharynx and extends along the E-shaped mesal edge of the maxillary stylet (Fig. 3A). Its posterior region is fused with the short and flattened maxillary lever (mxl) (Figs. 3A, 9I). The two upper extensions of the stylet each fit into a corresponding fold of the wing and lever, while the third ventral one encloses a protrusion (Figs. 8E–G, indicated by an arrow). Posterior to the compound eyes its proximal part forms a membranous connection to the ventral region of the head capsule (Fig. 9I). The wing and lever provide a guiding device for the maxillary stylet.

The functional complex of the salivary pump comprises the bowl-like part of the hypopharynx, the pumping chamber, the piston, the salivary glands, the salivary ducts and the retractor muscle of the piston. The membranous pumping chamber (pc) is anterodorsally linked with the efferent salivary duct (sdmx), which forms the con-

nection with the salivary channel of the maxillae (Figs. 6A, 8E). The duct lies above the hypopharynx and enters the salivary channel in the region of the base of the mandibular plate (Fig. 6A). The paired long and slender common afferent salivary ducts (sd) are fused anterad, just before they enter the pumping chamber anteroventrally (Figs. 6A, 8F). The common salivary duct originates in the cervical region where the principal and accessory duct fuse, enclosed by the principal gland (Fig. 8M,N). The principal duct (sd1) is very short (Fig. 8N) while the accessory duct (sd2) is long and slender and forms a loop in the middle part of the head capsule (Figs. 6A, 9K,M). The sac-shaped principal gland (sg1) is composed of few large cells with a circular arrangement (Figs. 6A, 9L). The cells are densely filled with secretion granules (se) enclosing a bean-shaped nucleus (n) (Fig. 9L,M). The thin tunica propria (tp) forms the external tissue layer (Fig. 9M). Innervations are not recognizable. Detailed information on the accessory gland is given in MIYAMOTO (1976) and COBBEN (1978).

The sclerotised piston (pis) is connected membranously with the pumping chamber (Figs. 6A, 8F). It is composed of a short ovoid anterior part and a long flattened posterior part with a bifurcated ending (Figs. 6A, 9I). The transition region to the ovoid part is strongly folded in cross section (Fig. 8G).

Musculature. M23 (Figs. 6A, 8H, 9K): one of the largest muscles of the head, O – lateroventrally on the postoccipital region, ventrad the strengthened part; I – laterally on the middle region of the piston, enclosing of the bifurcated ending; F – contraction results in an extension of the pumping chamber and influx of saliva from the salivary glands; relaxation pulls the piston back into the pumping chamber which pumps saliva through the salivary duct (sdmx) to the maxillary salivary channel. M24 absent.

Epipharynx

The epipharynx is not present as a clearly defined structure. It may be represented by a flat area of the caudal clypeal region. The density of the tissue in the caudoventral clypeal region is distinctly higher than in the surrounding medium. It is likely that this flattened agglomeration of cells is the epipharyngeal sense organ (eps) (Figs. 6, 8D). Some authors (e.g. CRANSTON & SPRAGUE 1961) also assigned the dorsal region of the food pump to the epipharynx.

Musculature. No musculature is associated directly with the epipharynx.

Pharynx

The pharynx is divided into two regions which are distinctly different anatomically and histologically. The precerebral part (“food pump”) has a wide lumen and reaches from the origin of the maxillary food channel to

the anterior part of the brain (prepharynx, pph) (Fig. 6A). It is followed by a “intracerebral” part with a distinctly narrowed lumen (pharynx *sensu stricto*, ph) (Fig. 9J). In cross section the precerebral pharynx appears U- to V-shaped. Ventrolaterally it is strongly sclerotised whereas the dorsal part forms a membranous cover which is prolonged as a tendon dorsally (Fig. 8E–G). The tendon is the attachment side for the anterior cibarial muscle bundles (Fig. 6A). In the posterior region the muscle inserts directly on the dorsal side of the pharynx (Fig. 9I). The transition to the tube-like “intracerebral” part is abrupt (Fig. 6A) and marked by the presence of a ring muscle layer (indicated by an arrow in Fig. 9J), which is less strongly developed in the posterior part.

Musculature. Pharyngeal muscles (M25–M30). Longitudinal muscles not recognizable. M25 (Figs. 6A, 8E): unpaired, V-shaped, O – dorsally on the roof of the head capsule, posterad the epistomal ridge; I – dorsally on the tendon of the precerebral pharynx; F – dilation of the cibarium. M26 (Figs. 6A, 8E): a paired delicate muscle, O – dorsally on the roof of the head capsule, posterad the epistomal ridge, laterad the O of M25; I – laterally on the anterior region of the precerebral pharynx; F – dilator. M27 (Figs. 6A, 8H, 9I): unpaired, V-shaped, O – dorsally on the roof of the head capsule, mesad the compound eyes, posterad the O of M25; I – with a tendon on the precerebral pharynx, posterad the I of M26; F – dilator. M28 absent. M29 absent. M30 (Figs. 6A, 8H, 9I): unpaired, O – dorsally on the incision between the anterior and middle part of the head capsule; I – dorsally on the posterior part of the prepharynx; F – dilator.

Brain

The brain is largely restricted to the middle part of the head capsule and nearly fills out its entire lumen (Fig. 6B). The cephalic part of the central nervous system is subdivided into the protocerebrum (pcr) and a compact complex comprising the deuto- and tritocerebrum and the subesophageal complex (dts). The protocerebrum is composed of two connected lateral lobes which cover the proximal region of the brain, and two short lobes (pcrlo) at the posterior end. The latter are directed caudad and reach the postoccipital region (Figs. 6B, 7, 9J). The lateral lobes provide a narrow passage (p) for the pharynx and aorta cephalica (Figs. 6B, 9J). The circumesophageal connectives are very broad, short and compact, and hardly recognizable as separate structures. The optic lobes (oplo) originate on the anterior region of the lateral protocerebral lobes (Figs. 7, 9I). A short nerve tract connects the ocellar lobes (oclo) to the dorsal side of the lateral lobes (Figs. 6B, 9J). The elongated unit formed by the deuto- and tritocerebrum and the subesophageal complex (dts) is distinctly separated from the first prothoracic ganglion (fg) by two short, mesally fused connectives (Figs. 6B, 9L–N). The paired labial nerves (lnv) originate ventrally in the middle region of the subesophageal complex (Figs. 6B, 8C, 9J). The paired antennal nerves (anv) arise

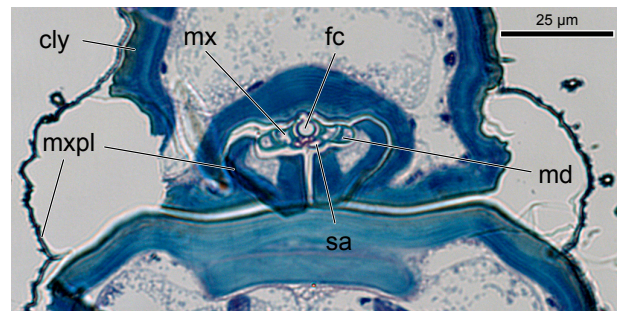


Fig. 10. *Systelloderes* sp.: head, cross section, plane of section anterad Fig. 8C. cly, clypeus; fc, food channel; md, mandible; mx, maxilla; mxpl, maxillary plate; sa, salivary channel.

anteriorly from the deutocerebral region mesad the optic lobes (Figs. 6B, 9I). In the same area the short frontal connectives originate which connect the protocerebral region with the arched frontal ganglion (fg) (Figs. 6B, 7). Two long nerves (cnv), extending into the clypeal region originate on the anterior part of the frontal ganglion. They end close to the assumed epipharyngeal sense organ (Figs. 6B, 7, 8H). The hypocerebral ganglion is not distinguishable. Maxillary and mandibular nerves could not be reconstructed precisely with the available section series.

A thin neural lamella (nl) forms the external cell layer of the brain, followed by a sparsely developed neurilemma (nr) composed of few flattened cells. A bark cell layer (bc) (GRAICHEN 1936) of variable thickness encloses the dense internal neuropil (np). The bark cell layer is distinct in the anterolateral region of the protocerebrum and the caudal lobes, reduced to a thin layer in the deuto-tritocerebrum-subesophageal-complex, strongly reduced in the circumesophageal connectives, and absent in the labial, antennal and clypeolabral nerves. The neuropil is less dense in the connectives and contains scattered single nuclei of the connective tissue (nct) (Fig. 9J–N).

Aorta cephalica and antennal hearts

The aorta (ao) is attached to the pharynx dorsally (Figs. 6, 9J). Anterad the middle part of the head capsule the lumen of the aorta widens (Fig. 7). It is shifted dorsad and situated between the bundles of the V-shaped cibarial dilators. The antennal hearts (ah) are placed in the dorsal region of the antennal socket (Fig. 7). The transition to the aorta cephalica could not be reconstructed precisely with the available section series.

3.2. *Cryptostemma waltli* (Dipsocoromorpha)

Like in the previous morphological section the head structures are treated in a morphology-based sequence. In some cases only differences to *Systelloderes* are pointed out.

Head capsule

The ellipsoid head capsule is prognathous. It is partly retracted into the prothorax (Figs. 11, 14). The dorsal and lateral areas bear a sparse vestiture of long and short setae (Fig. 11A,B). Pairs of cephalic trichobothria are not recognisable. The triangular vertex (vx) is not clearly separated from the flattened frons (fr) (Fig. 11A). The frons is separated from the clypeus by the epistomal ridge (epr) (Fig. 11B), which is less distinct than in *Systelloderes*. The compound eyes are located laterally, composed of fewer ommatidia than in *Systelloderes* and restricted to the posterior part of the head, close to the anterior margin of the prothorax (Fig. 11B). A thin sclerotised plate separates the anteromesal side of the eye from the adjacent region of the head capsule (indicated by arrows in Figs. 12A, 16G). The circumocular ridge (cor) is indistinct. Ocelli are absent. The genal area (ga) is adjacent to the anteroventral region of the compound eye (Fig. 11B). The anterior region of the head capsule is transformed into a ring-like bulge representing the bucculae (bu) (Figs. 11B,C, 16C–E). The antennal socket (as) lies between the bucculae and the genal area (Figs. 11B, 16F). Setose maxillary and mandibular plates are present dorsad the bucculae, between the antennal base and the clypeus, respectively. The maxillary plates (mxpl) are blunt cone-shaped sclerites separated from the bucculae by the ventral cleft (vc, see PARSONS 1968) (Figs. 11B, 16C). The mesal areas are slightly protruding inwards and form the ventral guiding device for the feeding stylets (Figs. 12, 16C). Their posterior regions are fused with the head capsule (Fig. 16C,D). The lora or mandibular plates (lor) are similar in shape to the maxillary plates but more pointed dorsally. They are separated from the former by the mandibular sulcus (msu) and from the clypeus by the clypeoloral cleft (clc) (Figs. 11B, 16C). The mesal edges are attached to the hypopharynx while the caudal ones are fused with the head capsule (Fig. 16C,D). In contrast to *Systelloderes* the genal suture is not recognizable. The anterior and mesal regions of the maxillary and mandibular plates are both covered by the clypeus (Fig. 16C). Subgena, subgenal ridges and the frontal and coronal (= epicranial) sutures are not distinguishable.

The ventral closure of the head capsule is formed by the “gular region” (gu). It is separated from the bucculae by a rim (Fig. 11C). The gular region is glabrous, except for two setae located mesally in the same plane as the compound eyes (Fig. 11B,C).

The dorsolateral area of the short postoccipital region is completely retracted into the prothorax (Figs. 12, 16I). The postoccipital ridge is not distinguishable. In contrast to the enicocephalid species, this region of the head does not form a ball-and-socket joint. The thickness of the lateral sides of the postoccipital region is partly increased (stout paired cuticular condyles, indicated by an arrow in Fig. 16I). The dorsal side is not transformed into a thin lip-like apodeme. The ventral region of the postoccipital region ends with the anterior margin of the prothorax and is not covered by the latter (Fig. 11C). The cervix is re-

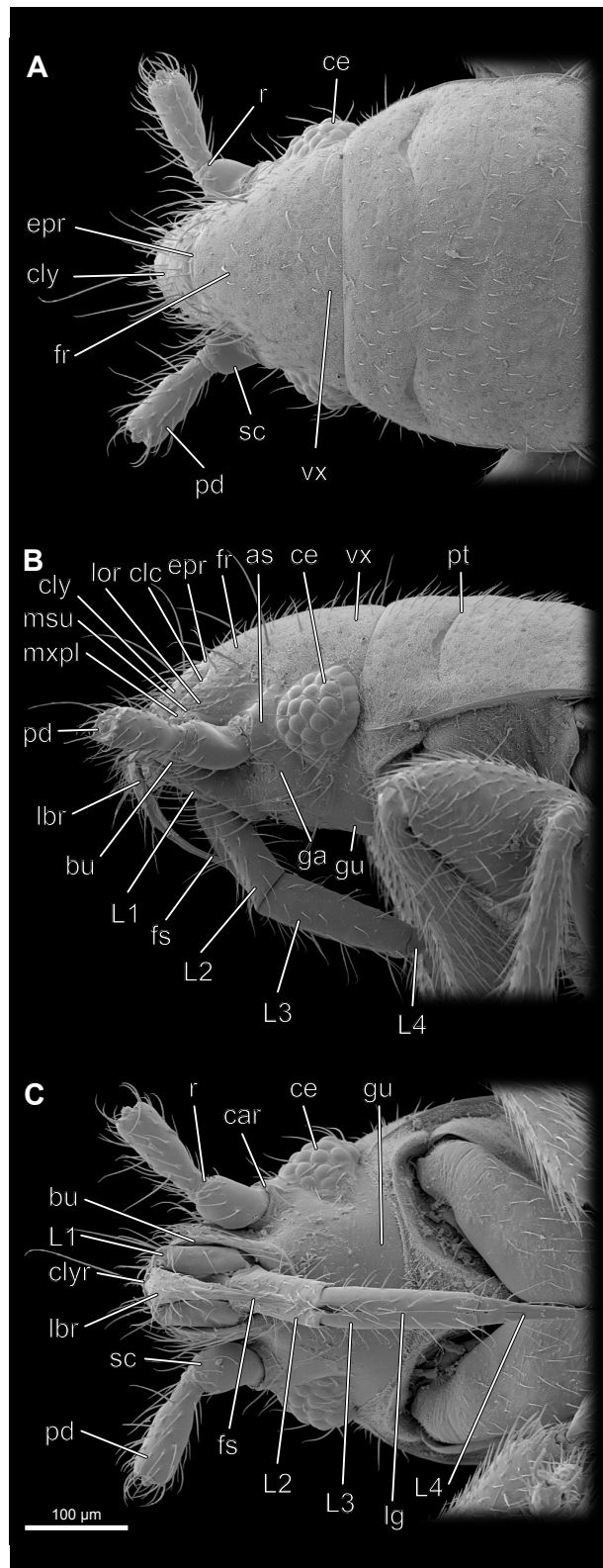


Fig. 11. *Cryptostemma walili* Fieber, 1860: head and thorax, basi- and distiflagellum omitted, SEM. **A:** dorsal view; **B:** lateral view; **C:** ventral view. as, antennal socket; bu, buccula; car, circumantennal ridge; ce, compound eye; clc, clypeoloral cleft; cly, clypeus; epr, epistomal ridge; fr, frons; fs, feeding stylets; ga, genal area; gu, gular region; L1–L4, labial segment 1–4; lbr, labrum; lg, labial groove; lor, lorum/mandibular plate; msu, mandibular sulcus; mxpl, maxillary plate; pd, pedicellus; pt, prothorax; r, ring-like structure between scapus and pedicellus; sc, scapus; vx, vertex.

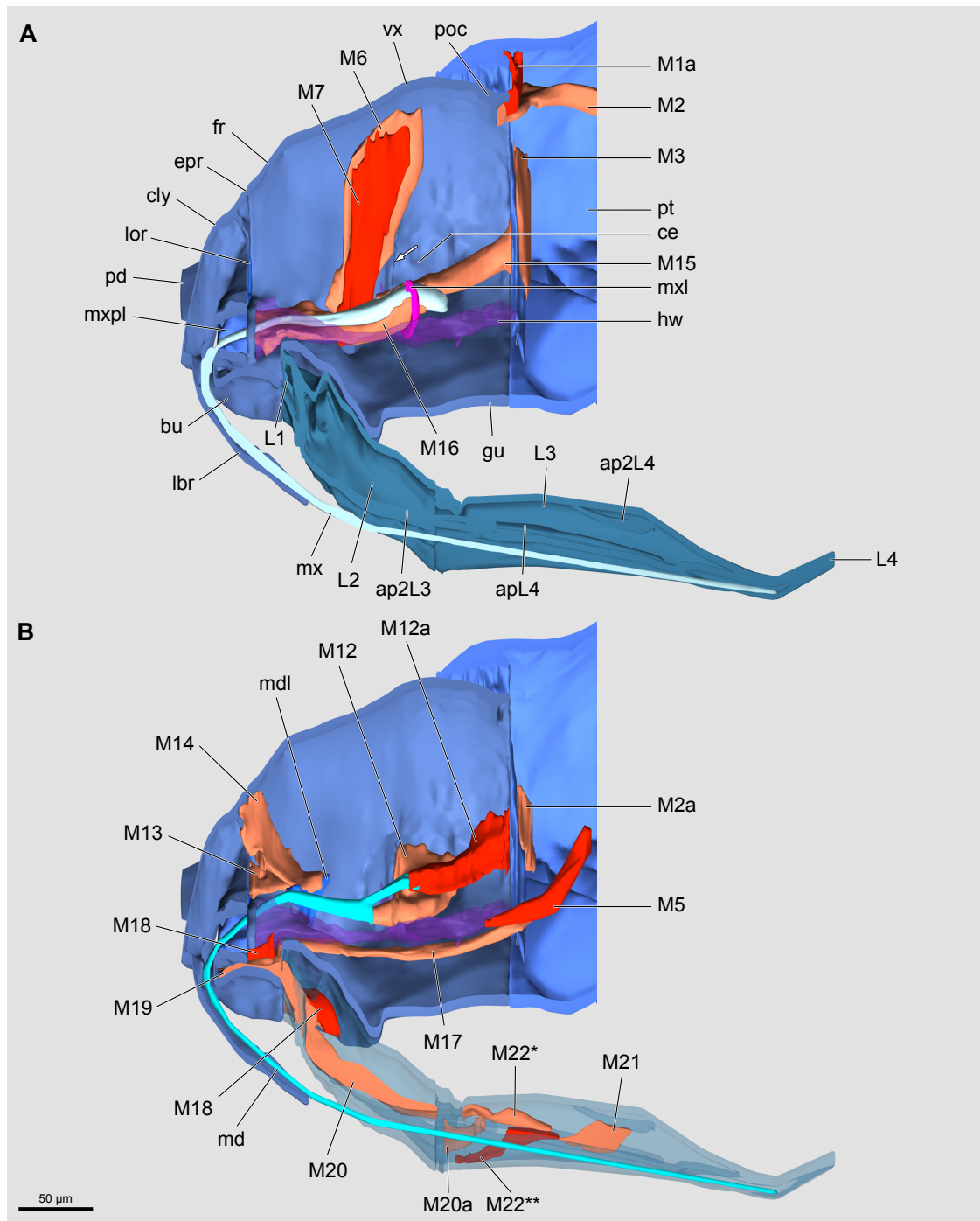


Fig. 12. *Cryptostemma waltli* Fieber, 1860: head and thorax, 3D-reconstruction, sagittal section, different muscles and feeding stylets shown (blue: sclerotization, red: musculature), labium in (B) semitransparent. ap2L3, unpaired bar-shaped apodeme of the 3rd labial segment; apL4, paired apodeme of 4th labial segment; ap2L4, unpaired apodeme of 4th labial segment; b, buccula; ce, compound eye; cly, clypeus; epr, epistomal ridge; fr, frons; gu, gular region; hw, hypopharyngeal wing (semitransparent); L1–L4, labial segment 1–4; lbr, labrum; lor, lorum/mandibular plate; M, muscle with appropriate number (number of muscle corresponds to number in text, Figs. 14–16, Table 1); md, mandible; mdl, mandibular lever; mx, maxilla; mxl, maxillary lever; mxpl, maxillary plate; pd, pedicellus; poc, postoccipital region; pt, prothorax; vx, vertex. Arrow in (A) indicates sclerotised plate of compound eye (see also Fig. 16G).

duced. The pronotal collar (see EMSLEY 1969) is absent in *Cryptostemma*.

Musculature. (M1–M5). M1 not distinguishable in *Cryptostemma*. M1a (Figs. 12A, 16I): larger than in *Systelloderes*, O – mesal area of the pronotum; I – mediodorsal region of the postocciput; F – depressor of the head.

M2 (Figs. 12A, 16I, J): O – mesonotum; I – dorsally on the postocciput; F – levator of the head. M2a (Figs. 12B, 16I): O – laterally on the pronotum; I – dorsomedially on the postocciput; F – levator of the head. M3 (Figs. 12A, 16I): O – mesal region of the pronotum; I – ventrolaterally on the postocciput; F – depressor of the head. M4

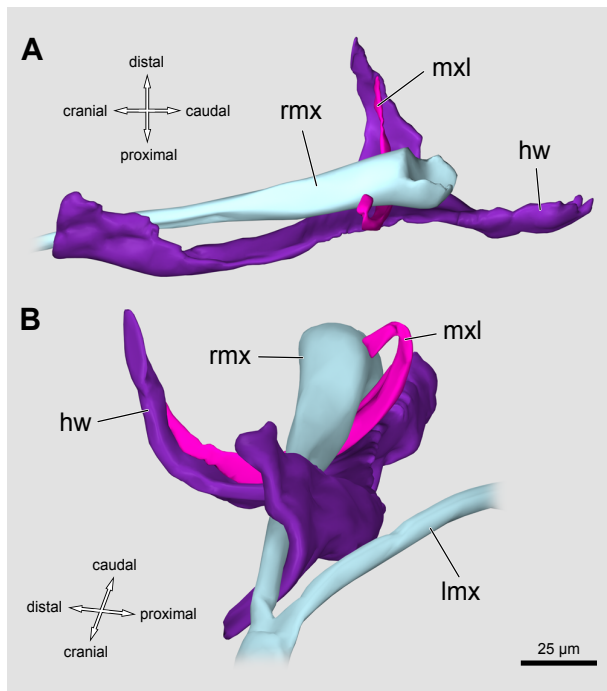


Fig. 13. *Cryptostemma waltli* Fieber, 1860: hypopharyngeal wing and maxillary lever, 3D-reconstruction. **A:** dorsolateral view; **B:** frontal view. hw, hypopharyngeal wing; lmx, left maxilla; mxl, maxillary lever; rmx, right maxilla.

absent. M5 (Figs. 12B, 16I, J): likely fused with M5b, O – anterad the profurcal arm; I – ventrally near the post-occipital region; F – depressor and retractor of the head. M5a absent.

Tentorium

The tentorium is completely reduced. Anterior and posterior tentorial pits are not developed. Endoskeletal elements not belonging to the tentorium are the hypopharynx, the hypopharyngeal wings, the piston of the salivary pump and the mandibular and maxillary lever, which are treated separately in the following chapters.

Clypeus and labrum

The rectangular and flat clypeus (cly) is not divided into an anteclypeus, paraclypeus and postclypeus. Its dorsal side is densely covered with long setae (Fig. 11A,B). The anterior part of its ventral region forms a longitudinal rim functioning as a guiding device for the stylets (Fig. 16B). Its posterior ventral region and the dorsal side of the hypopharynx together form a tongue-and-groove-joint (Fig. 16C).

In contrast to *Systemloderes*, the clypeus of *Cryptostemma* is directed more dorsoventrally (Figs. 11B, 12A). The triangular labrum follows this orientation. It is almost as long as the clypeus and bent in a ventrocaudal direction. The clypeo-labral ridge (clyr) is distinct (Fig.

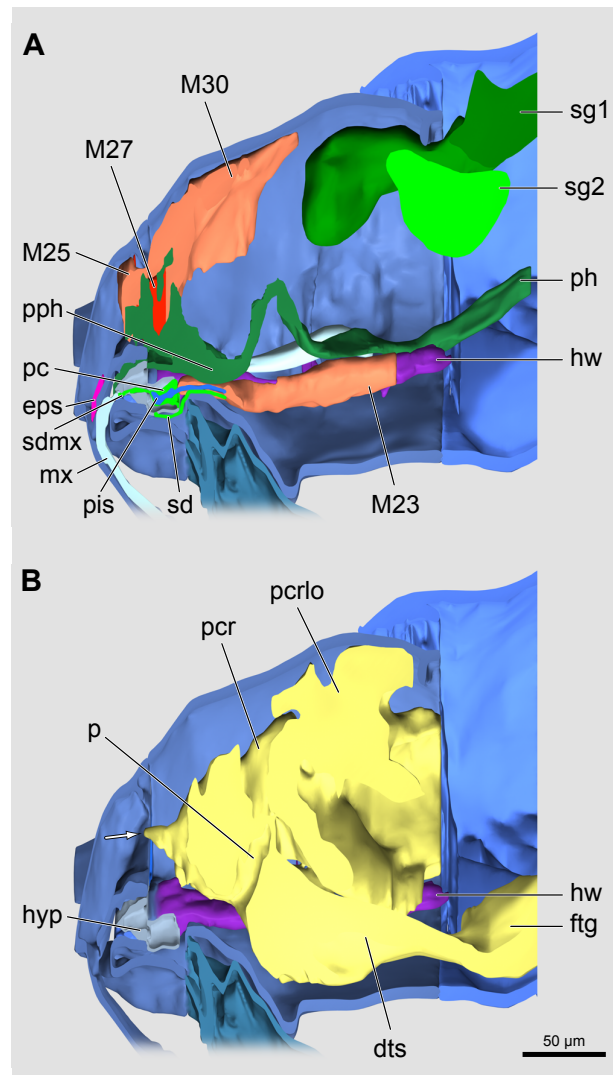


Fig. 14. *Cryptostemma waltli* Fieber, 1860: head and thorax, 3D-reconstruction, sagittal section, different muscles, alimentary system (A) and nervous system (B) shown (blue: sclerotization, dark green: pharynx, light green: salivary complex, red: musculature, yellow: nervous system). dts, deuto-tritocerebrum-subesophageal-complex; eps, epipharyngeal sense organ; ftg, first thoracal ganglion; hyp, hypopharynx; M, muscle with appropriate number (number of muscle corresponds to number in text, Figs. 12, 15, 16, Table 1); mx, maxilla; p, passage through brain for pharynx; pc, pumping chamber; pcr, protocerebrum; pcrlo, protocerebral lobe; ph, pharynx; pis, piston; pph, prepharynx; sd, common salivary duct; sdmx, salivary duct connecting pumping chamber with salivary channel of maxillae; sg1, principal gland; sg2, accessory gland. Arrow in (B) indicates extension of protocerebrum (see also Fig. 16D).

11C). The dorsal side of the clypeus is densely covered with setae. The clypeal longitudinal guiding rim continues on the ventral side (Fig. 16B,C). Due to the hypognathous placement of the tip of the labium, the labrum is not attached to the first and second labial segments (as in *Systemloderes*). A large cleft is present between these structures (Fig. 11B).

Musculature. No muscles are associated with the clypeus and the labrum. M10 and M11 absent.

The sclerotised mandibular lever (mdl) is a stout right angle. The arm which is attached to the stylet is elongated (type II of RIEGER 1976) (Fig. 12B). It is located posterad the lorum and attached to the mandible by its simple anterior apex (Fig. 16E,F). A longitudinal sclerotised stripe of cuticle is not present. The mandibular sac is indistinct. Mandibular glands are absent.

Musculature. Retractor and promoters of the mandibular stylet (M12–M14). M12 (Figs. 12B, 16G, H): O – laterally on the roof of the head capsule, posterad the compound eye; I – posterad the widening of the mandible; F – retractor. M12a (Figs. 12B, 16H): O – laterally on the postoccipital region, near the thickening of the cuticle; I – slender apodeme of the mandible; F – retractor. M12b: absent. M13 (Figs. 12B, 16C–E): O – lorum; I – laterally on the distal side of the mandibular lever; F – protractor. M14 (Figs. 12B, 16D–F): O – dorsally on the border region of clypeus and head capsule; I – laterally on the distal side of the mandibular lever, posterad the I of M13; F – protractor.

Maxilla

The maxillae consist mainly of the very elongate laciniae. The palp and galea are absent. The proximal elements appear indistinguishably fused, without a recognizable detachment of the lacinia from the stipes. The laciniae, probably together with the parts corresponding with the cardo and stipes (mx), form a pair of hollow, slender stylets. They are similar to the mandibles in position and shape. However, they end abruptly posteriorly with their widened part (Figs. 12A, 16H). The linkage of the anterior two thirds resulting in the formation of the food channel and salivary channel is similar to that of *Systelloderes* (Fig. 16H). The E-shaped structure reaches the region posterad the antennal socket (Fig. 16F). The maxillary sac is not distinct. The posterior region of the maxilla is mesally connected with a crescent-shaped maxillary lever (Fig. 12A). The proximal part of this sclerotised structure is strongly bent laterad and attached to the mesal side of the maxilla, while the distal region follows the lateral extension of the hypopharyngeal wing (Figs. 13, 16H). Maxillary glands are not present.

Musculature. Retractor and promotor of the maxillary stylet (M15, M16). M15 (Figs. 12A, 16H, I): O – laterally on the distal postoccipital region, ventrad the increased sclerotization, ventrad the O of M12a; I – dorsally on the maxillary stylet, posterad the E-shaped structure; F – retractor. M16 (Figs. 12A, 16C, G, H): one of the largest intrinsic cephalic muscles, O – on the maxillary plate; I – ventrolaterally on the base of the stylet; F – promotor.

Labium

The tube-like, four-segmented labium forms the ventral closure of the anterior part of the head capsule (Fig. 11B,C). The feeding stylets lie within this tube (Fig.

12). In its resting position it is caudally oriented (Fig. 11B). In contrast to *Systelloderes* the entire surface of the labium is covered with a sparse vestiture of long setae (Fig. 11B,C). The labial groove (lg) is present on the ventral side of segments two to four (Fig. 16G). The four segments are separated from each other by articulation membranes (Fig. 11B,C). The basal segment (L1) is shorter than the others, only weakly sclerotised, and not in contact with the feeding stylets (Figs. 11B, 16C,D). Its ventral area is strongly folded and clearly separated from the second segment (Fig. 11C, 16A). The second (L2) and third segments (L3) are similar in shape. The base of L2 is partly retracted into the basal segment. In contrast to *Systelloderes*, no distinct apodemes are present. The third segment (L3) is the longest and 1.5 as long as L2 (Fig. 11B,C). Its base is partly retracted into L2 and bears an apodeme on both sides. The floor of the proximal labial groove is strongly sclerotised and forms a bar-shaped apodeme anteriorly as in *Systelloderes* (ap2L3) (Figs. 12A, 15, 16H). A distinct linkage of the edges of the labial groove is not present (Fig. 16H–J). The cone-shaped apical labial segment (L4) is half as long as L2 (Fig. 11C). Two bar-shaped apodemes (apL4) originate on its base and reach almost the distal end of L3 (Figs. 12A, 15, 16J). Additionally, an unpaired bar-shaped apodeme is present (ap2L4). It originates on the dorsal base of L4 and is attached to the dorsal side of the middle region of L3. A distinct apical row of sensilla is not present (Fig. 11C). Intercalary sclerites are also missing.

Musculature. Extrinsic and intrinsic labial muscles (M17–M22). M17 (Figs. 12B, 15, 16D): largest extrinsic labial muscle, O – ventrolaterally on the postoccipital region; I – distally on the base of L1; F – extensor of the labium. M17a (Figs. 15, 16B,C): O – anterior part of the bucculae; I – anterior base of L2; F – flexor of the labium (simultaneous contraction) or rotator. M18 (Figs. 12B, 15, 16D): O – anterior border region of the hypopharyngeal wing and the mesal wall of the maxillary plate; I – posterior base of L2; F – flexor of the labium (simultaneous contraction) or rotator. M19 (Figs. 15, 16C,E): unpaired, O – mesally on the anterior region of the bucculae L2; I – with its bifurcated posterior region on the anterior base of L2, mesad the I of M17; F – flexor of the labium. M20 (Figs. 12B, 15, 16F, H): unpaired, O – anterior base of L2, posterad the I of M19; I – dorsally on the base of L3; F – flexion of L3 and L4. M20a (Figs. 12B, 15): O – laterally on the base of L3; I – laterally on the posterior part of the apodeme ap2L3; F – contraction likely results in an extension of L2. M21 (Figs. 12B, 16J): unpaired, stout muscle, O – ventrally on the apodeme ap2L4; I floor of the labial groove in L3; F – pulls the floor of the labial groove upwards and closes the lateral sides of the labial groove, probably also extension of L4 (connection over the labial floor). M22* (Figs. 12B, 16I): first partition of M22, O – dorsally on the anterior side of L3; I – dorsally on the apodemes apL4; F – flexion (simultaneous contraction) or rotator of L4. M22** (Figs. 12B, 16I): second partition of M22, O – ventrolaterally on the anterior side of L3; I – ven-

trally on the apodemes apL4; F – flexion (simultaneous contraction) or rotator of L4.

Hypopharynx, salivary pump and salivary glands

The sclerotised hypopharynx (hyp) is subdivided into a three-cornered anterior part (“hypopharyngeal lobe”) and a bowl-shaped posterior part (Fig. 14A). The former is dorsally enclosed by the clypeus, laterally by the mandibular and maxillary plates, and ventrally by the bucculae and the dorsal base of the first labial segment (Fig. 16C). The anterodorsal side of the hypopharynx forms a rim (Fig. 16C). In combination with the ventral extension of the clypeus, it forms the transition between the prepharynx and the food channel formed by the maxillary stylet. Its ventrolateral sides bear two paired indentations functioning as the dorsal guiding device for the feeding stylets (Fig. 16C). The duct connecting the pumping chamber with the salivary channel of the maxillae (sdmx) lies within the ventral hypopharyngeal region (Figs. 14A, 16C). The proximal areas of the anterior part are fused with the mesal walls of the maxillary plates laterally and the prepharynx dorsally (Fig. 16D). The posterior part encloses the membranous pumping chamber (pc) (Figs. 14A, 16D).

The hypopharyngeal wings (hw) are more complex than those in *Systelloderes*. They are formed by lateral extensions of the anterior hypopharyngeal part (Fig. 16C,D). The mesoventral wall of the maxillary plate and the ventral wall of the lorum are partly integrated in the anterior region of the wings, the latter on the dorsal side (Fig. 16D). Consequently, the wings have a dorsoventral orientation in this region of the head (Figs. 13B, 16D). The two lateral rims of the hypopharynx are guiding devices for the feeding stylets, with the posterior part interacting only with the maxillae (Figs. 13A, 16D,E). Anterodorsally the orientation of the hypopharyngeal wings switches from dorsoventral to transverse (Figs. 13A, 16G). In the ocular region, the wing is more planar and forms a triangular extension laterally which is directed dorsad and located close to the internal ocular plate (Figs. 13, 16G, H). In its posterior region the wing tapers and switches back to a dorsoventral orientation (Figs. 13B, 16I). Its posterior end is located in the border region of the head capsule and prothorax (Figs. 14B, 16I).

The structure of the functional complex of the salivary pump is similar to that of *Systelloderes*. However, the duct “sdmx” in *Cryptostemma* is located more ventrally in relation to the hypopharynx. The connection between the salivary duct “sd” and the principal gland (sg1), the principal duct and the accessory duct could not be reconstructed precisely with the available section series (Fig. 14A). The sac-shaped elongated principal gland (sg1) is composed of few large cells and situated in the border region between the head capsule and prothorax (Figs. 14A, 16H, J). The cells are densely filled with secretion granules (se) which enclose a bean-shaped large

nucleus (n) (Fig. 16H). The thin tunica propria (tp) forms the external layer (Fig. 16H). A second gland (sg2) of vesicular structure, possibly homologous with the accessory gland, is present posteroventrad the principal gland. According to MIYAMOTO (1967) it is located “below the principal gland”. This gland is also sac-shaped but composed of smaller cells. Associated nerves are not recognizable.

The sclerotised piston (pis) is similar to that of *Systelloderes* (Fig. 14A). However, the posterior end is blunt and not bifurcated. The transition of the ovoid part to the plate-like part is smooth without a distinct folding in cross section (Fig. 16E).

Musculature. M23 (Figs. 14A, 16E, H): one of the largest muscles of the head, O – mesal side of the posterior and middle region of the hypopharyngeal wing; I – laterally on the middle region of the piston; F – contraction results in an extension of the pumping chamber and influx of saliva from the salivary glands; relaxation pulls the piston back into the pumping chamber, thus pumping saliva through the salivary duct (sdmx) to the maxillary salivary channel. M24 absent.

Epipharynx

The epipharynx is not present as a clearly defined structural unit. It may represent a flat area of the caudal clypeal region. The density of the tissue in the anteroventral clypeal region is distinctly higher than in the surrounding areas. This flattened agglomeration of cells likely represents the epipharyngeal sense organ (eps) (Figs. 14A, 15, 16B).

Musculature. No muscles are directly associated with the epipharynx.

Pharynx

The cephalic digestive tract is divided into two regions which distinctly differ morphologically and histologically. The short precerebral part, i.e. the prepharynx, has a wide lumen and reaches from the origin of the maxillary food channel to the level of the antennal socket (prepharynx, pph) (Fig. 14A). As in *Systelloderes* it is V-shaped in cross section with a sclerotised ventral floor and a membranous dorsal wall with a strongly sclerotised tendon attached to it (Fig. 16C–E). The prepharynx is partly covered by the protocerebrum (pcr) dorsally (Fig. 16F). The transition to the tube-shaped pharynx (ph) is enclosed by the anterior part of the brain and surrounded by a delicate ring muscle layer (Fig. 16G). In this region the pharynx is strongly bent and appears like a reversed “V” in cross section (Fig. 14A). The posterior pharyngeal section is shifted to the right side of the head whereas the esophagus lies in the median plane in the thoracic segments (Figs. 14A, 16I).

Musculature. Pharyngeal muscles (M25–M30). Longitudinal muscles not recognizable. M25 (Figs. 14A,

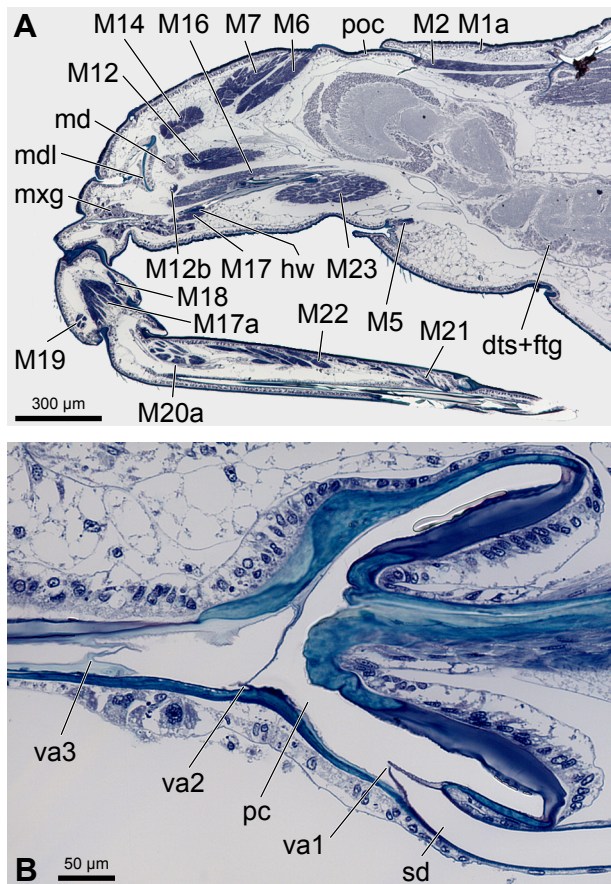


Fig. 17. *Gerris* sp.: **A:** head and thorax, right half, parasagittal longitudinal section. **B:** detail of salivary pump, sagittal longitudinal section. dts+ftg, fused complex of deutocerebrum, tritocerebrum, subesophagealganglion and first thoracic ganglion; hw, hypopharyngeal wing; M, muscle with appropriate number (number of muscle corresponds to number in text and Table 1); md, mandible; mdl, mandibular lever; mxg, maxillary gland; pc, pumping chamber; poc, postoccipital region; sd, afferent salivary duct; va, valve with appropriate number.

16C): unpaired, V-shaped, O – dorsally on the posterior region of the clypeus; I – dorsally on the prepharyngeal tendon; F – dilator of the cibarium. M26 not distinguishable as a separate unit. M27 (Figs. 14A, 16C): unpaired, V-shaped, O – dorsally on the posterior region of the clypeus, posterad the O of M25; I – dorsally on the prepharyngeal tendon, posterad the I of M25; F – dilator. M28 absent. M29 absent. M30 (Figs. 14A, 16D, G): unpaired, interrupted by two extensions of the protocerebrum anteriorly, O – frontal region; I – dorsally on the middle region of the prepharynx; F – dilator.

Brain

Due to the very small size of the head the brain appears greatly compressed. As in *Systelloderes* it is subdivided into the protocerebrum (pcr) and a compact complex comprising the deutocerebrum and tritocerebrum and the subesophageal complex (dts) (Fig. 14B).

The protocerebrum (pcr) is composed of two extensions anterad which are likely the origin of the innervation of the epipharyngeal sense organ (Figs. 14B, 16D, indicated by arrows) and two dorsal lobes (pcrlo) covering the proximal region of the brain (Figs. 14B, 16G). The latter are caudally directed and reach the postoccipital region (Fig. 14B). In contrast to *Systelloderes* the narrow passage for the pharynx is very short. The circumesophageal connectives are not distinguishable. The optic lobes are indistinguishably fused with the lateral sides of the protocerebral lobes (Fig. 16H). The globular unit formed by the deutocerebrum and tritocerebrum and the subesophageal complex (postcerebral complex, dts) is distinctly separated from the first prothoracic ganglion (ftg) by short and flat, mesally fused connectives (Fig. 16G–J). The paired antennal nerves (anv) arise from the anterior region of the postcerebral complex (Figs. 15, 16F). The frontal ganglion and the hypocerebralganglion are not recognizable as separate structures. Maxillary, mandibular and labial nerves could not be reconstructed precisely with the available section series.

As in *Systelloderes*, the thin neural lamella forms the external cell layer of the brain. The neurilemma is composed of single flattened cells and is even more sparsely developed than the one in *Systelloderes*. A bark cell layer (bc) of variable thickness encloses the dense internal neuropil (np) (Fig. 16E–G). The bark cell layer is very distinct in the anterodorsal region of the protocerebrum and the caudal lobes and reduced to few scattered cells in the proximal parts of brain. The density of the neuropil is uniform in the different parts of the brain.

Aorta cephalica and antennal hearts

Not clearly recognizable in the available section series, possibly reduced.

3.3. *Gerris* sp. (Gerromorpha)

The external and internal cephalic morphology was already described in detail in MATSUDA (1961) and ANDERSEN (1982). Consequently, we only present missing information here, especially on the muscle system (Fig. 17A). The cephalic muscles are numbered following the system used for *Systelloderes* and *Cryptostemma* (see Table 1). A distinctive feature of the salivary pump is the presence of three valves (Fig. 17B, va1–va3). The first valve (va1) is composed of two anteriorly directed flaps. They are placed at the anterior end of the common afferent salivary duct (sd) where it merges with the pumping chamber. The second valve (va2) on the floor of the salivary pump is formed by a large dorsal flap and a very small ventral one. Both are also anteriorly directed. The third pair of valve flaps (va3) is inserted directly anterior to the origin of the salivary duct, which is connected to

the salivary canal of the maxilla. Both are posteriorly directed. The valves obviously function passively as muscles are lacking.

4. Discussion

4.1. Morphology and homology

Systelloderes, *Cryptostemma* and *Gerris* differ strongly in their external and internal head morphology even though some heteropteran ground plan features are preserved in all three groups. We compared skeletal and muscular features potentially relevant in a phylogenetic context to conditions found in other heteropteran groups (Tables 1, 2) using extensive literature data (see Table 3). Antennal features were adopted from ZRZAVÝ (1990) and features of the digestive tract from MIYAMOTO (1961). Information on the feeding stylets was provided by COBBEN (1978).

Inconsistent designations for different cephalic areas were used by different authors dealing with Heteroptera (see below, e.g. “postclypeus”). Consequently we strictly follow the terminology used for head structures in SCHUH & SLATER (1995) and in a detailed study on the generalized Grylloblattodea (WIPFLER et al. 2011). The head of Hemiptera is generally composed of the vertex, the variously shaped frontoclypeal region, semicircular to quadrangular mandibular plates, triangular maxillary plates, mandibular and maxillary stylets, the tube-like labial rostrum, and a triangular labrum (SINGH 1971; SCHUH & SLATER 1995). Enicocephalomorpha are the only infraorder with the head capsule distinctly constricted behind the compound eyes which is combined with a distinctly swollen portion bearing the ocelli (autapomorphy) (see also WHEELER et al. 1993). The subdivision of the clypeus in ante-, post- and paraclypeus is indistinct in *Systelloderes*, Dipsocoromorpha, Ochteridae (RIEGER 1976), Gerromorpha (MATSUDA 1960; ANDERSEN 1982), Nepidae (Nepomorpha) (HAMILTON 1931) and Saldidae (PARSONS 1962), whereas the substructures are very clearly separated in other families such as for instance Corixidae (BENWITZ 1956: paraclypeal structures as “Clypeus-Seitenflügel”). The “postclypeus” of *Saldula* (PARSONS 1962), *Gerris* (Gerridae) (CRANSTON & SPRAGUE 1961), Gerromorpha (ANDERSEN 1982) and Schizopteridae (Dipsocoromorpha) (EMSLEY 1969) is in fact the morphological frons, and consequently the “frons” in *Saldula* (PARSONS 1962) is the vertex in the stricter sense (according the sequence from cranial to caudal: labrum, clypeolabral ridge, anteclypeus fused with postclypeus, epistomal ridge, frons, vertex). Assuming that, the epistomal ridge is homologous to the “clypeal fold” in Schizopteridae (EMSLEY 1969), to the

Table 1. Proposed homology of the musculature of *Systelloderes*, *Cryptostemma* and *Gerris* with other representatives of Hemiptera. Unclear homologies set in parentheses, (---) muscle absent, (?) not mentioned by the author or further figures and descriptions for a clear conclusion are absent in the cited works. ² “F” referring to number of musculature of thorax, “H” referring to number of musculature of head. ³ Muscles were not named in BENWITZ (1956); therefore, the nomenclature of the enicocephalid species is applied.

	<i>Systelloderes</i>	<i>Cryptostemma</i>	<i>Ochterus</i> (RIEGER 1976)	<i>Corixa</i> (BENWITZ 1956)	<i>Gelastocoris</i> (PARSONS 1958, 1959, 1960a)	<i>Lethocerus</i> (PARSONS 1968)	<i>Nepa</i> (HAMILTON 1931; RIEGER 1976)	<i>Gerris</i>	<i>Hydrometra</i> (SPRAGUE 1956)	<i>Saldula</i> ² (PARSONS 1962, 1963)	<i>Triatoma</i> (BARTH 1952a,b 1953a,b; RIEGER 1976)	<i>Dysdercus</i> (KUMARI 1955; KHAN 1972)	<i>Hackeriella</i> (SPANGENBERG et al. 2013)	<i>Aphis</i> (WEBER 1928, 1929)
M1	M1		TM10b	rot cap1	TM10b	10	?	M1	M3	T10	?	?	M1	OdvM
M1a	M1a	TM1	TM1	ret cap1	TM1	1	2nd cranial flexor	M1a	M2	T1	?	?	M1a	—
M2	M2	TM3	TM3	ret cap2	TM3	3	?	M2	M1	T3	?	?	M2	Odlm
M2a	M2a	TM10a	TM10a	rot cap2	TM10a	6a	?	M2a	M7	—	?	?	—	—
M3	M3	TM2	TM2	depr cap	TM2	2	cranial flexor	M3	M10	T2	?	?	(M3)	Oism
—	—	—	—	—	—	—	?	—	—	—	?	?	M4	m.tent2
M5	M5	TM6	TM6	ret cap3	TM6	6B	?	M5	M6	T6	?	?	M5	OvIm4
—	—	KM24	KM24	Ømu	KM24	H24	?	—	?	—	?	?	M5a	—
M5b	M5b	TM7	TM7	lev cap	TM7	7	?	M5b	M6	T7	?	?	—	OvIm4
M6	M6	KM21	KM21	dep isc	KM21	21	?	M6	?	H21	MUI4	depressor	M6	ant1
M7	M7	KM20	KM20	lev?sc	KM20	20	?	M7	?	H20	MUI3	levator	M7	ant4
M8	M8	KM23	KM23	M8 ³	KM23	H23	?	M8	?	H23	?	intrinsic muscles	M8	ant2

M9	M9	KM22	M9 ³	KM22	—	?	M9	?	H22	?	intrinsic muscles	M9	ant3
—	—	(TM11)	—	—	—	?	—	?	—	—	—	M10	—
—	—	—	—	—	—	?	—	?	—	—	—	M11	m. lam. mand1+2
M12	M12	KM10	retr mand	KM10	H10	KM10	M12	?	H10	—	retractors/RMD1	M12	m. retr. mand1+2
M12a	M12a	KM11	—	KM11	H11	—	M12a	?	H11	MU11	retractors/RMD2	—	—
M12b	—	—	—	—	—	?	M12b	?	—	—	—	—	—
M13	M13	KM8	protr mand	KM8	H8	KM8	M13	?	H8	MU15	protractors/ PMD	M13	m. protr. mand
M14	M14	KM9	—	KM9	—	—	M14	?	H9	MU8	—	M14	—
M15	M15	KM13	retr max	KM13	H13	KM13	M15	?	H13	MU9+ MU10	retractors/RMX	M15	m. retr. maax1+2
M16	M16	KM12	protr max	KM12	H12	KM12	M16	?	H12	MU6+ MU7	protractors/ PMX1+2	M16	m. protr. max1+2
M17	M17	KM2b	add lb1	—	H2B	KM2b	M17	?	H2	MU5	ADL1	M17	m. add1
M17a	M17a	KM1	MuFa	KM1	H1	KM1	M17a	?	H1	MU16	(ABL)	—	m. abd1+2
M18	M18	KM2a	add lb2	KM2	H2A	KM2a	M18	?	H1.5	MU4	(ABL)	M18	m. add2
M19	M19	KM3	depr lb1	KM3	H3B	KM3	M19	?	H3	—	—	M19	m. add4
—	—	—	—	—	H3A	?	—	?	—	—	?	—	—
M20	M20	KM4	—	KM4	H4	KM4	M20	?	H4	MUD proximal	ADL2	M20	m. add3
M20a	M20a	KM5	trans lb	KM5	H5	KM5	M20a	?	H5	—	ADL3	—	m. trans2-4
M21	M21	KM6	—	KM6	H6	KM6	M21	?	H6	MUD distal	TLB1	M21	m. trans5
M22*	M22*	KM7a	(depr lb2)	KM7	H7	KM7	M22*	?	H7	MUL	RLB	M22	m. abd3
M22*	M22*	KM7b	(depr lb2)	KM7	H7	KM7	M22**	?	H7	MUL	RLB	M22	m. abd3
M23	M23	KM25	retr pist	KM25	H25	KM25	M23	?	H25	MU12	DSS1+2	M23	m. retr. pist2
—	—	—	—	—	—	?	—	?	—	—	—	M24	(m. dil. cup1)
M25	M25	KM14	abd lr	KM14	H14	KM14	M25	?	H14	MU1	—	M25	m. dil1
M26	M26	KM15	dil cib	KM15	H15	KM15	M26	?	—	MU2	DSP1	M26	m. dil2
M27	M27	KM16	dil buc	KM16	H16	KM16	M27	?	H16	MU2	DSP2	M27	m. dil3
—	—	KM19	dil ph3 d	KM19	H19	?	—	?	H19	MU17	?	M28	—
—	—	KM18	dil ph 3 v	KM18	H18	?	—	?	H18	—	?	M29	m. depr. phar.
M30	M30	KM17+ KM17a	dil ph1 +2+m dilator oris	KM17+ KM17	H17+ H17a	KM17+ KM17a	M30	?	H17+ H17a	MU3	DPH	M30	—
—	—	—	—	—	—	—	—	?	—	—	?	—	m. tent1
—	—	—	—	—	—	—	—	?	—	—	?	—	m. protr. max1
—	—	—	—	—	—	—	—	?	—	—	?	—	m. retr. pist1
—	—	—	—	—	—	—	—	?	—	—	?	—	m. dil. cup2
—	—	—	—	—	—	—	—	?	—	—	?	—	m. dil. cup3
—	—	—	—	—	—	—	—	?	—	—	?	—	m. dil. cup4
—	—	—	—	—	—	—	—	?	—	—	?	—	m. dil. cup5
—	—	—	—	—	—	—	—	?	—	—	?	—	m. trans1
—	—	—	—	—	—	—	—	?	—	—	?	—	m. add5
—	—	—	—	—	—	—	—	?	—	—	?	—	OvIm1
—	—	—	—	—	—	—	—	?	—	—	?	—	OvIm2
—	—	—	—	—	—	—	—	?	—	—	?	—	OvIm3

“clypeal cleft” in Gerromorpha (ANDERSEN 1982, see also his statement on page 31: “[...] divide the clypeal region into an anteclypeus [...] and a postclypeus [...] “frons” of many authors.”) and to the “frontal suture” in *Gerris* (CRANSTON & SPRAGUE 1961). In *Saldula* (PARSONS 1962) the border of frons (“postclypeus”) and clypeus (“anteclypeus”) is indicated in fig. 3 but not labeled. The bucculae usually partly enclose the base of the labium. In *Saldula* (“gular lobe”) (PARSONS 1962) they are vestigial and completely absent in Enicocephalidae, Corixidae (BENWITZ 1956), Gerromorpha (ANDERSEN 1982). Genae partially reaching beyond the maxillary plates anteriorly probably only occur in Enicocephalidae and Reduviidae (WEIRAUCH 2008). An apomorphic feature generally characterizing Heteroptera (autapomorphy) is the presence of a gula (e.g. SPOONER 1938).

The median ocellus is always missing, whereas absence or presence of the paired ocelli varies among and within the higher groups of Heteroptera. Both character states occur for instance in Schizopteridae (Dipsocoromorpha) (EMSLEY 1969), Enicocephalomorpha (ŠTYS 1995a) and Gerromorpha (ANDERSEN 1982), and are frequently, but not always, correlated with a shortening of the hemelytron (brachypterous to apterous).

The postoccipital condyles are usually well developed, but reduced in *Hydrometra* (SPRAGUE 1956) and *Dysdercus* (KUMARI 1955; KHAN 1972). According to GRIFFITH (1945) they are vestiges of the cervical sclerites, whereas HAMILTON (1981) interpreted the two ventral spurs as “posterior tentorial bars”. We follow RIEGER (1976) and ANDERSEN (1982) who interpreted them as simple extensions of the postoccipital region.

The homology of the “dorsal apodemes” of *Saldula* (PARSONS 1962) is ambiguous. Their specific position suggests that they may represent anterior tentorial arms. Accordingly, the corresponding indentations in *Saldula* (PARSONS 1962), the small pits associated with the clypeal connectives (“sclerotised connections [...] which run from the clypeus to the dorsolateral margins of the [foodpump]”) in *Gelastocoris* (PARSONS 1959), and the vestigial anterior pits in *Lethocerus* (PARSONS 1968) may be identified as anterior tentorial grooves. The hypopharyngeal wing of *Nepa* is flanked by an additional paired sclerotised structure referred to as “anterior arm of tentorium” (HAMILTON 1931). Its relative position suggests that it may be in fact homologous with the anterior arm. However, the assumed anterior arms do not originate on the epistomal ridge (= “frontal suture” of HAMILTON 1931) but laterally between the clypeus and lora.

Three pairs of cephalic trichobothria are present in Leptopodomorpha, Gerromorpha and in some groups of Cimicomorpha (SCHUH & SLATER 1995). An additional fourth pair is present in Gerridae, arguably an autapomorphy of the family. The gerromorph cephalic trichobothria clearly differ from the “usual” flat articulation by their origin in a deep funnel-shaped pit (autapomorphy) (ANDERSEN 1982) (character 12 in the phylogenetic analysis). WEIRAUCH (2012) documented “three pairs of very long and stout setae” for the dipsocoromorph species *Vorago-*

coris schuhi Weirauch (Schizopteridae). However, they differ not distinctly from the surrounding setae and are arguably no cephalic trichobothria in a stricter sense.

The antenna of Heteroptera varies considerably in its shape and composition. In the ground plan it is composed of four elongate tubular segments separated from each other by intraflagelloides (ZRZAVÝ 1990). The preflagelloides (pedicello-flagellar intersegmental sclerites) also occur in Thysanoptera and Coleorrhyncha (ZRZAVÝ 1990), but they are extremely reduced or absent in *Hackeriella* (SPANGENBERG et al. 2013). Although the antenna of Enicocephalomorpha is largely conforming to the assumed ancestral state, the condition of the prepedicellite and its affiliation to the ground plan remains uncertain. It is absent in Nymphocorinae and Alienatinae (see ZRZAVÝ 1990). So far, the “scapus sclerites” are only documented for *Systelloderes* which is treated here (autapomorphy). According to ZRZAVÝ (1990), there are two antennal synapomorphies for Dipsocoromorpha – “the preflagelloid of type IV and the tubulous extension of the pedicellar apex into the pedicello-flagellar articulation”. A ring-like desclerotised region of the basiflagellite and distiflagellite (“R-structure”) occurs in Dipsocoromorpha, Gerromorpha, Leptopodomorpha and Cimicomorpha (ZRZAVÝ 1990). However, its shape is highly variable in Dipsocoromorpha and Gerromorpha and it can be absent in the former. Apparently, the entire antennal morphology is of limited value for phylogenetic reconstruction on a higher level due to its extreme variability within the infraorders.

Hydrometra and *Systelloderes* are the only taxa with the retractor muscles of the piston originating on the posterior cephalic region. This is likely due to the extremely elongated head and the limited capacity of the hypopharyngeal wings to extend.

The presence of maxillary glands in the ground plan of Heteroptera is questionable (SCHUH & SLATER 1995). They are absent in *Systelloderes*, *Cryptostemma*, *Hydrometra*, *Saldula*, and *Triatoma*. The presence of mandibular glands in the ground plan of Heteroptera is also questionable. They are documented for *Oncopeltus* (Lygaeidae, Pentatomomorpha) (LINDER 1956) and also for some Aphididae (SAXENA & CHADA 1971).

Triturating devices of the food pump for crushing and grinding particles in the food stream occur only in infraorders mainly or exclusively containing carnivorous species. However, they are absent in the predacious *Systelloderes*, *Cryptostemma*, *Gerris*, *Hydrometra* and the blood-feeding *Triatoma*. According to COBBEN (1978) it is unclear why some groups evolved these nodes and ridges and others apparently did not.

The homology of cephalic muscles of members of Heteroptera and the other hemipteran lineages is still greatly impeded by a severe lack of reliable data, especially for Auchenorrhyncha. In the following, selected ambiguous muscles of representatives of Heteroptera, Coleorrhyncha (*Hackeriella*) and Sternorrhyncha (*Aphis*) are discussed, based on the results presented here, the detailed treatment of the head morphology of *Hacke-*

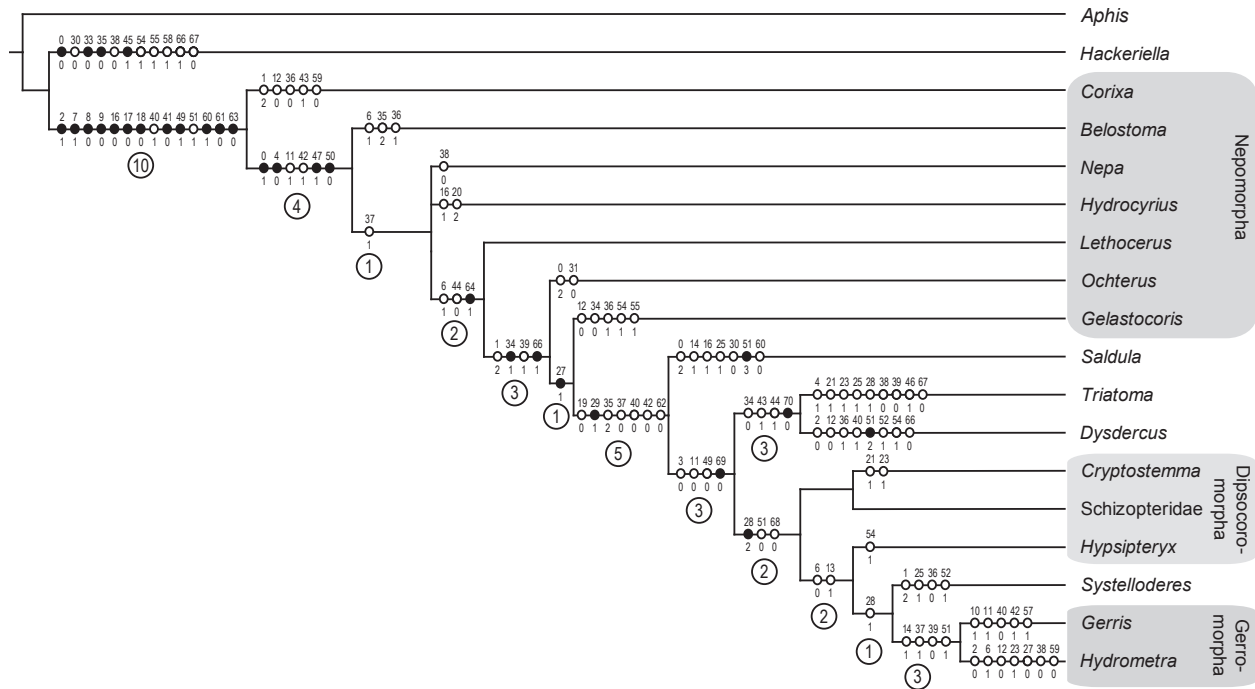


Fig. 18. Phylogenetic diagram [16 heteropteran taxa and *Aphis* (Sternorrhyncha) and *Hackeriella* (Coleorrhyncha)] generated with nona and tree analyses using new technology (single minimum length tree). Full circles show unambiguous apomorphic character states, white circles show homoplasious changes and encircled numbers give Bremer support values. The numbers correspond to those in chapter 4 and Table 2.

riella in SPANGENBERG et al. (2013), and previously published anatomical studies on members of Heteroptera and *Aphis*. The homology of **M3** (*M. pronoti secundus*, terminology of PARSONS 1959, 1960a and RIEGER 1976) of Heteroptera and Coleorrhyncha (*Hackeriella*) is problematic. The muscle originates on the pronotum and inserts on the posterior margin of the head capsule in Heteroptera (and *Aphis*), but on the apodeme of the maxillary plate in *Hackeriella*. The homology would imply a shift of the insertion. **M5a** (*M. dilatator oris glandulae capitis*) of *Hackeriella* is likely equivalent to the dilatator muscle of the maxillary gland in Heteroptera. The gland is probably generally absent in Coleorrhyncha, and the muscle is a vestigial unpaired structure. Nevertheless, the similar position suggests homology. The labial abductor muscles ABL of *Dysdercus fasciatus* are located in a similar position as **M17a** and **M18**. However, the description in KHAN (1972) does not allow an unambiguous interpretation. KHAN (1972) documented transverse muscles TLB2 in the fourth labial segment of *Dysdercus fasciatus*. These are apparently very small fibers distinctly differing from muscles functioning as a compact unit. They are also present in the enicocephalid species but extremely small. The interpretation of the labial muscles of *Corixa* is complicated by the reduced structure of the labium. This applies for instance to the depr lb2 (*m. depressor labii secundus*) which may or may not be homologous with **M22** (*M. retractor segmenti ultimi labii*). Both **M24** of Coleorrhyncha and *m. dil. cup1* (*m. dilatator primus cupulae*) of *Aphis* originate on the hypopharynx (WEBER 1928), which suggests

possible homology. However, in contrast to the condition in *Aphis* **M24** inserts on the afferent common salivary channel and not directly on the pumping chamber. The homology of the two muscles would imply a shift of insertion in *Hackeriella*. As already stated in SPANGENBERG et al. (2013), the structure of the musculature of the food pump is highly variable and the separation of defined sets of muscles (**M25–M27**, **M30**) is difficult (i.e. fig. 15 in PARSONS 1968). In particular this concerns the subdivision or fusion of the two partitions of **M30** (*M. dilatator cibarii quartus*). Therefore, we treat the posterior set of the cibarial retractors as a single morphological entity.

A hypothesis on homology of muscles listed and named in the systems of von KÉLER (1963), FRIEDRICH & BEUTEL (2008), and WIPFLER et al. (2011) was already presented in SPANGENBERG et al. (2013) and is shown here in Table 1.

4.2. Phylogeny and character evolution

A cladistic analysis based on 71 head characters of 16 heteropteran terminals and *Hackeriella* and *Aphis* as outgroups (Table 2) yielded two minimum length trees (L: 175) with the strict consensus (L: 176) as shown in Fig. 18. Apart from the well supported monophyly of Heteroptera, the branching pattern is in contrast to other currently favored hypotheses. Some results, in particular the

Table 2. Character states of adults of selected taxa of Heteroptera with the outgroups *Aphis* and *Hackeriella* (below on this page; numbers correspond to those in text and Fig. 18), and List of Characters (following page).

	0	1	2	3	4	5	6	7	8	9	0	1	2	3	4	5	6	7	8	9	0	1	2	3	4	5	6	7	8	9	0	1	2	3	4	5	
	0	0	0	0	0	0	0	0	0	0	1	1	1	1	1	1	1	1	1	1	1	2	2	2	2	2	2	2	2	2	3	3	3	3	3	3	
Sternorrhyncha: <i>Aphis</i>	2	1	0	-	1	0	0	0	1	1	0	0	1	1	0	-	1	1	1	0	0	0	-	0	-	0	-	0	-	?	1	0	0	1	4	1	
Coleorrhyncha: <i>Hackeriella</i>	0	0	0	-	1	1	0	0	1	1	0	0	1	1	0	-	1	1	1	1	2	0	-	-	-	0	-	0	-	-	0	0	0	0	-	0	
Enicocephalomorpha: <i>Systelloderes</i>	1	2	1	0	0	-	0	1	0	0	0	0	1	1	0	-	0	0	0	0	1	0	-	0	-	1	0	1	1	1	1	1	1	1	2	1	
Dipsocoromorpha: <i>Cryptostemma</i>	1	0	1	0	0	-	1	1	0	0	0	0	1	0	0	-	0	0	0	0	1	1	0	1	0	0	-	1	2	1	1	1	1	1	1	2	
Dipsocoromorpha: <i>Hypsiteryx</i>	1	0	?	?	?	0	-	0	1	0	0	0	0	1	1	0	-	?	?	?	?	0	1	0	-	0	-	0	-	1	2	1	?	?	?	?	
Dipsocoromorpha: Schizopteridae	1	-	?	?	?	0	-	1	1	0	0	0	0	1	0	0	-	?	?	?	?	0	1	0	-	0	-	0	-	1	2	1	?	?	?	?	
Nepomorpha: <i>Ochterus</i>	2	2	1	1	0	-	1	1	0	0	1	1	1	0	0	-	0	0	0	1	1	0	-	0	-	0	-	0	-	0	1	0	1	1	1	1	
Nepomorpha: <i>Corixa</i>	2	2	1	0	1	1	0	1	0	0	0	0	0	0	0	-	0	0	0	1	1	0	-	0	-	0	-	0	-	0	1	1	?	1	0	?	
Nepomorpha: <i>Gelastocoris</i>	1	2	1	1	0	-	1	1	1	0	0	1	0	0	0	-	0	0	0	1	1	0	-	0	-	0	-	1	3	0	1	1	1	1	0	1	
Nepomorpha: <i>Lethocerus</i>	1	0	1	1	0	-	1	1	1	0	1	1	1	0	0	-	0	0	0	1	1	0	-	0	-	0	-	0	-	0	1	1	1	1	2	?	
Nepomorpha: <i>Belostoma</i>	1	0	1	1	0	-	1	1	0	0	0	1	1	1	0	-	0	0	0	1	1	0	-	0	-	0	-	0	-	0	1	0	1	1	2	2	
Nepomorpha: <i>Hydrocyrius</i>	1	0	?	?	?	0	-	0	1	0	0	0	1	1	0	0	-	?	?	?	?	1	1	0	-	0	-	0	-	0	1	?	1	1	2	?	
Nepomorpha: <i>Nepa</i>	1	0	?	?	?	0	-	0	1	0	0	1	1	1	1	0	-	1	0	0	1	2	0	-	0	-	0	-	0	-	0	?	1	1	1	2	?
Gerromorpha: <i>Gerris</i>	1	0	1	1	0	-	0	1	0	0	1	1	1	1	1	0	0	0	0	0	1	0	-	0	-	0	-	1	1	1	1	1	1	1	3	1	
Gerromorpha: <i>Hydrometra</i>	1	0	0	-	0	-	1	1	0	0	0	0	0	1	1	0	0	0	0	0	1	0	-	1	1	0	-	0	-	1	1	1	1	1	3	-	
Leptopodomorpha: <i>Saldula</i>	2	2	1	1	0	-	1	1	1	0	0	1	1	0	1	1	1	0	0	0	1	0	-	0	-	1	0	1	0	1	0	1	1	1	1	2	
Cimicomorpha: <i>Triatoma</i>	1	2	1	0	1	0	1	1	0	0	0	0	1	0	0	-	0	0	0	0	1	1	1	1	2	1	1	1	1	1	1	1	1	1	0	2	
Pentatomomorpha: <i>Dysdercus</i>	1	0	0	-	0	-	1	1	0	0	0	-	0	0	0	-	0	0	0	0	1	0	-	0	-	0	-	0	-	1	0	1	1	1	1	0	2

	6	7	8	9	0	1	2	3	4	5	6	7	8	9	0	1	2	3	4	5	6	7	8	9	0	1	2	3	4	5	6	7	8	9	0		
	3	3	3	3	4	4	4	4	4	4	4	4	4	4	4	5	5	5	5	5	5	5	5	5	5	6	6	6	6	6	6	6	6	6	6	7	
Sternorrhyncha: <i>Aphis</i>	2	0	1	1	0	1	0	2	1	0	0	0	1	0	1	0	1	0	0	0	0	0	0	0	1	0	1	0	1	0	0	0	1	0	1	1	
Coleorrhyncha: <i>Hackeriella</i>	2	0	0	0	0	1	0	2	1	1	0	0	1	0	1	0	1	1	1	1	0	1	1	1	0	1	1	1	0	0	1	0	1	1	1		
Enicocephalomorpha: <i>Systelloderes</i>	0	0	1	1	0	0	0	2	0	-	1	1	0	0	0	0	2	0	0	0	1	0	0	1	1	0	0	0	1	1	1	1	0	0	1		
Dipsocoromorpha: <i>Cryptostemma</i>	1	0	1	1	0	0	0	2	0	-	0	1	1	0	0	0	1	0	0	0	1	0	0	1	0	1	1	1	0	0	0	1	0	1	0	0	
Dipsocoromorpha: <i>Hypsiteryx</i>	?	0	1	?	?	?	0	2	?	?	?	?	?	?	?	0	1	0	1	?	?	?	?	?	?	?	?	?	?	?	?	?	?	?	?	?	
Dipsocoromorpha: Schizopteridae	?	0	1	?	?	?	0	0	-	?	?	?	?	?	?	0	1	0	0	0	1	0	0	0	1	0	1	1	?	?	?	?	?	?	?	?	
Nepomorpha: <i>Ochterus</i>	2	1	1	1	1	0	1	2	0	-	0	1	1	1	0	1	1	0	0	?	?	?	?	?	?	?	?	?	?	?	?	?	?	?	?	?	
Nepomorpha: <i>Corixa</i>	0	0	1	0	1	0	0	1	1	0	0	0	1	1	1	1	1	0	0	0	1	0	0	1	0	1	0	1	0	0	0	0	1	1	1		
Nepomorpha: <i>Gelastocoris</i>	1	1	1	1	1	0	1	2	0	-	0	1	1	1	?	1	1	0	1	1	1	0	0	1	1	0	1	0	1	0	1	1	1	1	1		
Nepomorpha: <i>Lethocerus</i>	?	1	1	0	1	0	1	2	0	-	0	1	1	1	0	1	1	0	0	0	1	1	0	1	1	0	1	0	1	0	0	1	1	1	1		
Nepomorpha: <i>Belostoma</i>	1	0	1	0	1	0	1	2	1	0	0	1	1	1	0	1	1	0	0	?	?	?	?	?	?	?	?	?	?	?	?	?	?	?	?	?	
Nepomorpha: <i>Hydrocyrius</i>	?	1	0	0	?	0	1	2	1	0	0	?	?	?	?	?	1	0	0	?	?	?	?	?	?	?	?	?	?	?	?	?	?	?	?	?	
Nepomorpha: <i>Nepa</i>	?	1	1	0	1	0	1	2	1	0	0	1	1	1	0	1	1	0	0	0	1	1	0	1	?	?	?	?	?	?	0	?	0	1	?	?	
Gerromorpha: <i>Gerris</i>	2	1	1	0	1	0	1	2	0	-	1	1	1	0	0	1	1	0	0	0	1	1	1	1	1	0	0	0	1	1	1	1	0	0	1		
Gerromorpha: <i>Hydrometra</i>	2	1	0	0	0	0	2	0	-	1	1	0	0	0	1	1	0	0	0	1	0	0	0	1	0	1	0	1	?	?	?	?	?	?	?		
Leptopodomorpha: <i>Saldula</i>	2	0	1	1	0	0	0	2	0	-	0	1	1	1	0	3	1	1	0	?	?	?	?	?	?	0	0	0	0	1	0	1	1	1	1		
Cimicomorpha: <i>Triatoma</i>	2	0	0	0	0	0	1	1	0	1	1	1	1	0	0	1	1	1	0	?	?	?	?	?	?	?	?	0	?	?	?	?	?	?	?	?	
Pentatomomorpha: <i>Dysdercus</i>	1	0	1	1	1	0	0	1	1	0	0	1	1	0	0	2	2	1	1	0	1	?	?	?	?	?	?	?	?	0	1	0	0	1	?	?	?

paraphyly of Nepomorpha appear very unlikely. It is apparent that cephalic features alone are insufficient for a clarification of the relationships of the major lineages of Heteroptera. Consequently, we used different published phylogenies to evaluate our set of characters and to discuss different scenarios. In the following the characters are indicated in the text in bold and in parentheses. The numbers correspond to those in Table 2 and Figs. 18 and 19.

Heteroptera is supported as a clade by 12 cephalic apomorphies in our analysis, i.e. the presence of cuticular condyles on the postocciput (**2**) (implying reversal in *Dysdercus*), the presence of a gula (**7**); the absence of the posterior and anterior tentorial pits (implying reversals in *Saldula*, *Gelastocoris* and *Lethocerus*; homol-

ogy not fully clarified, see above) (**8**, **9**); the absence of the tentorium (with possible reversal in the case of the anterior arms of *Nepa* and *Saldula*) (**16**, **17**, **18**); the origin of the labium on the anterior part of the head capsule (**41**); the presence of triturating devices (with reduction in several infraorders, see below and COBEN 1978) (**49**); the presence of M2a (M. proepisternopostoccipitalis secundus) (**60**) and the absence of M4 (depressor of the head, connecting the pronotum and the posterior tentorial arms) (**61**) and M11 (loral apodeme-postclypeal muscle) (**63**).

Hypotheses based on different data sets were presented by MAHNER (1993), WHEELER et al. (1993), SHCHERBAKOV & POPOV (2002), XIE et al. (2008), and LI et al. (2012b). We mapped our character data on three al-

List of characters

- 0 orientation of base of mouthparts relative to head: (0) posteriorly or posteroventrally = hypognathous; (1) anteriorly = prognathous; (2) ventrally = orthognathous
- 1 number of ocelli: (0) 0; (1) 3; (2) 2
- 2 cuticular condyles of postocciput: (0) absent; (1) present
- 3 shape and number of postoccipital condyles: (0) 2 processes; (1) 2 short + 2 long processes
- 4 subdivision of clypeus: (0) absent; (1) present
- 5 classification of clypeal subdivision: (0) subdivided in ante- and postclypeus; (1) additional paraclypeus
- 6 bucculae: (0) absent; (1) present
- 7 gula: (0) absent; (1) present
- 8 anterior tentorial pits: (0) absent; (1) present
- 9 posterior tentorial pits: (0) absent; (1) present
- 10 epicranial (=coronal) suture (adults): (0) absent; (1) present
- 11 frontal suture (adults): (0) absent; (1) present
- 12 epistomal ridge (separates clypeus from frons): (0) absent; (1) present
- 13 genal suture (separates lorum from remainder of head capsule): (0) absent; (1) present
- 14 pairs of cephalic trichobothria: (0) absent; (1) present
- 15 origin of cephalic trichobothria: (0) in a deep pitlike depression; (1) in a flat depression
- 16 anterior tentorial arms: (0) absent; (1) present
- 17 posterior tentorial arms: (0) absent; (1) present
- 18 corpotentorium: (0) absent; (1) present
- 19 antenna folded under head, received in a groove formed by genae: (0) absent; (1) present
- 20 number of antennomeres of flagellum: (0) 5 or more; (1) 4; (2) 3
- 21 basiflagellite equipped with R-Structure (ZRZAVÝ 1990): (0) absent; (1) present
- 22 type of R-Structure of basiflagellite (ZRZAVÝ 1990): (0) Bf(RVI); (1) Bf(RI)
- 23 distiflagellite equipped with R-Structure (ZRZAVÝ 1990): (0) absent; (1) present
- 24 type of R-Structure of distiflagellite (ZRZAVÝ 1990): (0) Df(RVI); (1) Df(RV); (2) Df(RI)
- 25 intercalary sclerite between scapus and pedicellus (“prepedicellite, pp”) (ZRZAVÝ 1990): (0) absent; (1) present
- 26 types of prepedicellite (ZRZAVÝ 1990): (0) pp(I); (1) pp(II)
- 27 intercalary sclerite (“preflagelloid, pf” or “prebasiflagellite, pb”) between antennomeres 2 and 3 (ZRZAVÝ 1990): (0) absent; (1) present
- 28 type of preflagelloid or prebasiflagellite (ZRZAVÝ 1990): (0) pf(I); (1) pf(II); (2) pf(IV); (3) pb
- 29 intercalary sclerite (“intraflagelloid, if”) between antennomeres 3 and 4 (ZRZAVÝ 1990): (0) absent; (1) present as if(I)
- 30 origin of extrinsic antennal muscles (M6, M. depressor scapi + M7, M. levator scapi): (0) anterior armstentorium; (1) head capsule;
- 31 protrusion of the proximal mandibular part in a long and slender apodeme or tendon: (0) absent; (1) present
- 32 shape of mandibular stylets in lateral view: (0) linear; (1) boomerang-shaped
- 33 mandibular lever (“Protraktorarm” of WEBER 1928): (0) absent; (1) present
- 34 shape of mandibular lever (characters 0–2 from RIEGER 1976): (0) equilateral triangle; (1) acute triangle, arm attached to mandible elongated; (2) acute triangle, arm attached to mandible elongated directed caudally; (3) quadrangular; (4) bar-shaped
- 35 formation of salivary canal: (0) by indentation of right maxilla; (1) by indentation of left maxilla; (2) mutual or variable in entire labial length
- 36 shape of maxillary stylets in cross-sectional view: (0) compressed dorso-ventrally; (1) compressed laterally; (2) circular
- 37 setae at tip of maxilla: (0) absent; (1) present
- 38 barb-like structures at tip of maxilla: (0) absent; (1) present
- 39 maxillary lever: (0) absent; (1) present
- 40 maxillary glands (“cephalic glands”): (0) absent; (1) present
- 41 origin of labium: (0) anterior part of head capsule; (1) cervical region
- 42 intercalary sclerites between 3rd and 4th labial segment (1 pair): (0) absent; (1) present
- 43 number of labial segments: (0) 1; (1) 3; (2) 4
- 44 sensilla at apex of labial rostrum: (0) absent; (1) present
- 45 sensilla grouping: (0) one group; (1) two rows
- 46 interlocking of the edges of the labial groove: (0) absent; (1) present
- 47 orientation of hypopharynx (including pumping chamber): (0) dorso-ventral; (1) cranio-caudal
- 48 origin of retractor muscle of piston (M23, M. retractor pistilli): (0) posterior region of head capsule; (1) hypopharyngeal wing
- 49 pharyngeal triturating devices (“striated plates”; “Kauapparat”): (0) absent; (1) present
- 50 distinct bent (dorso-ventral orientation to cranio-caudal) of pharynx: (0) absent; (1) present
- 51 principal salivary gland: (0) obscurely bi-lobed; (1) distinctly bi-lobed; (2) four-lobed; (3) single-lobed
- 52 structure of accessory gland: (0) vesicular; (1) tubular
- 53 structure of principal gland: (0) aciniform; (1) irregular
- 54 length of principal duct: (0) short; (1) long
- 55 triangular processes of tritocerebrum: (0) absent; (1) present
- 56 fusion of subesophageal ganglion with brain (to dts): (0) absent; (1) present
- 57 fusion of subesophagealganglion or dts with first thoracic ganglion: (0) absent; (1) present
- 58 frontal ganglion: (0) distinct; (1) indistinct, reduced in size
- 59 circumesophageal connectives: (0) elongate; (1) short and broad
- 60 M2a (M. proepisterno-postoccipitalis secundus): (0) absent; (1) present
- 61 M4 (depressor of the head, connecting the pronotum and the posterior tentorial arms): (0) absent; (1) present
- 62 M5a (M. dilatator oris glandulae capitis): (0) absent; (1) present
- 63 M11 (loral apodeme-postclypeal muscle): (0) absent; (1) present
- 64 M12a (M. retractor setae mandibularis secundus): (0) absent; (1) present
- 65 M12b (M. retractor setae mandibularis tertius): (0) absent; (1) present
- 66 M14 (M. protractor setae mandibularis secundus): (0) absent; (1) present
- 67 M20a (M. transversalis labii secundus): (0) absent; (1) present
- 68 M28 (M. dilatator postpharyngis dorsalis): (0) absent; (1) present
- 69 M29 (M. dilatator postpharyngis ventralis): (0) absent; (1) present
- 70 M19 (M. transversalis labii primus): (0) absent; (1) present

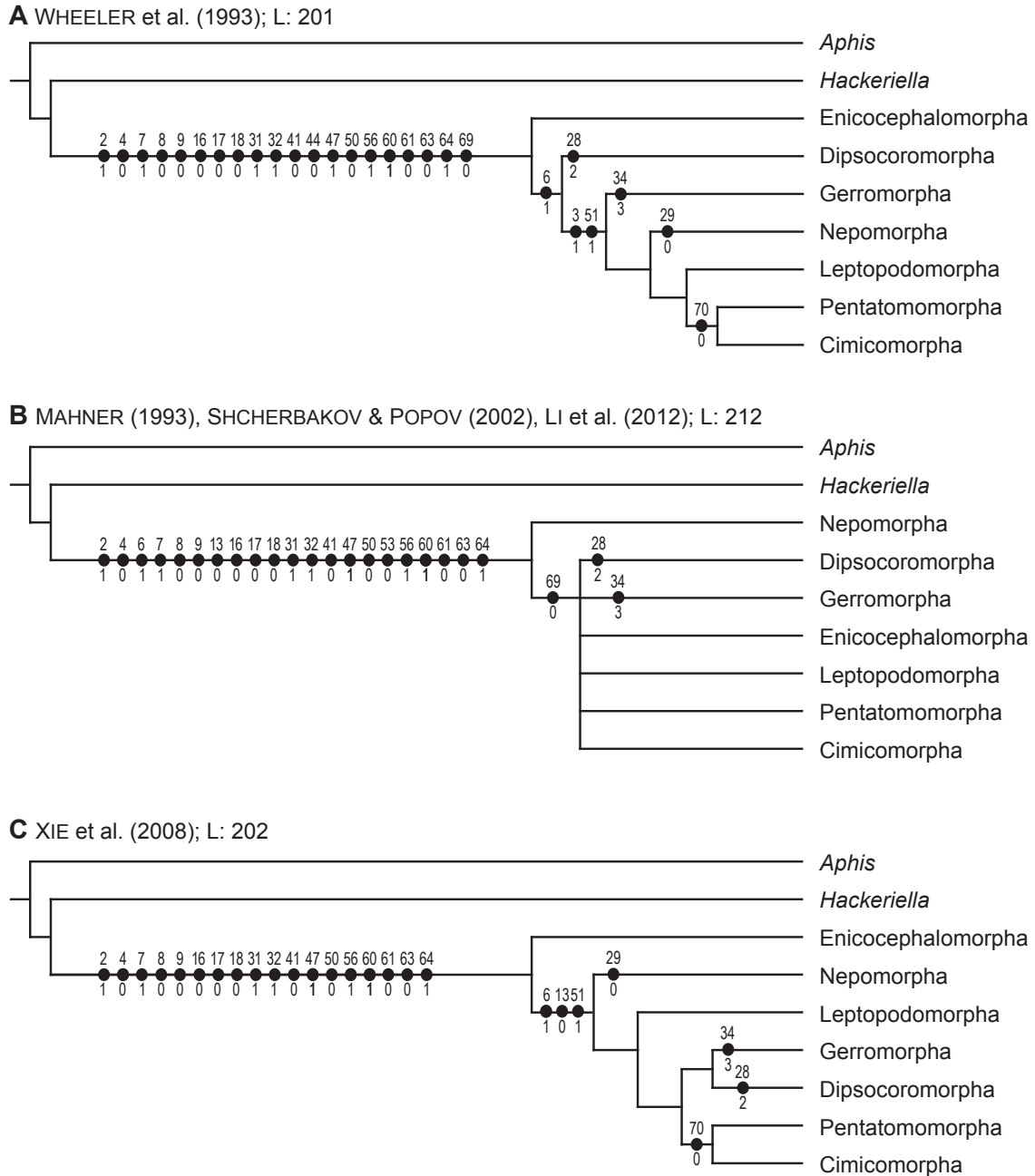


Fig. 19. **A:** phylogeny after WHEELER et al. (1993) (modified); **B:** phylogeny after MAHNER (1993), SHCHERBAKOV & POPOV (2002) and LI et al. (2012b) (modified); **C:** phylogeny after XIE et al. (modified). Full circles show unambiguous apomorphic character states, white circles for homoplasious changes not shown. The numbers correspond to those in chapter 4 and Table 2.

ternative topologies using Winclada (Fig. 19). The most parsimonious hypothesis is that of WHEELER et al. (1993, fig. 5), which required 201 steps (Fig. 19A), whereas 202 and 212 were required under the phylogenies suggested by XIE et al. (2008) (Fig. 19C) and MAHNER (1993) (Fig. 19B), respectively. The monophyly of Heteroptera is supported in the case of WHEELER et al. (1993) by 20 cephalic autapomorphies (Fig. 19A), in the case of MAHNER (1993) by 21 (Fig. 19B), and in the scenario of XIE et al. (2008) by 18 (Fig. 19C). In contrast, there are only single or very few apomorphies supporting major infraordinal branches, i.e. those supporting relationship between the infraorders. In the tree of WHEELER et al. (1993) (Fig.

19A), Euheteroptera (Heteroptera excl. Enicocephalomorpha) are supported by the presence of distinct bucculae (6), monophyletic Dipsocoromorpha by the presence of the preflagelloid antennal type IV (28), Neoheteroptera (Euheteroptera excl. Dipsocoromorpha) by the presence of paired cuticular condyles of the postocciput (3) and distinctly bi-lobed principal glands (51) (Fig. 19A), and Gerromorpha by the presence of cephalic trichobothria originating in a deep pit-like depression (15, not displayed in Fig. 19A) and a quadrangular mandibular lever (34). No cephalic features support Panheteroptera (Neoheteroptera excl. Gerromorpha) (Fig. 19A). Nepomorpha is supported by the absence of the intraflagelloid between

Table 3. List of taxa and corresponding literature used for morphological comparison and phylogenetic reconstruction.

Taxa	Literature
Dipsocoromorpha	
<i>Hypsiteryx</i> sp. (Dipsocoridae)	ŠTYS 1970
Schizopteridae	EMSLEY 1969
Nepomorpha	
<i>Ochterus marginatus</i> (Latreille, 1804) (Ochteridae)	RIEGER 1976
<i>Corixa punctata</i> (Illiger, 1807) (Corixidae)	BENWITZ 1956
<i>Gelastocoris oculatus</i> (Fabricius, 1798) (Gelastocoridae)	PARSONS 1958, 1959, 1960a,b
<i>Lethocerus uhleri</i> (Montandon, 1896) (Belostomatidae)	PARSONS 1968
<i>Belostoma</i> sp. (Belostomatidae)	VERMA et al. 1973; SWART & FELGENHAUER 2003
<i>Hydrocyrius columbiae columbiae</i> Spinola (Belostomatidae)	KOPELKE 1978
<i>Nepa cinerea</i> Linnaeus, 1758 (Nepidae)	HAMILTON 1931; RIEGER 1976
Gerromorpha	
<i>Gerris</i> sp. (Gerridae)	MATSUDA 1960; CRANSTON & SPRAGUE 1961; ANDERSEN 1982
<i>Hydrometra martini</i> Kirkaldy, 1900 (Hydrometridae)	SPRAGUE 1956; ANDERSEN 1982
Leptopodomorpha	
<i>Saldula pallipes</i> (Fabricius, 1794) (Saldidae)	PARSONS 1962, 1963
Cimicomorpha	
<i>Triatoma infestans</i> Klug, 1834 (Reduviidae)	BARTH 1952a,b, 1953a,b; RIEGER 1976
Pentatomomorpha	
<i>Dysdercus koenigii</i> Fabricius (Pyrrhocoridae)	KUMARI 1955
<i>Dysdercus fasciatus</i> Signoret (Pyrrhocoridae)	KHAN 1972
Outgroups	
<i>Aphis fabae</i> Scopoli, 1763 (Sternorrhyncha, Aphididae)	WEBER 1928, 1929; FORBES 1977
<i>Hackeriella veitchi</i> (Hacker, 1932) (Coleorrhyncha, Peloridiidae)	SPANGENBERG et al. 2013

antennomeres three and four (**29**). A potential additional nepomorphan autapomorphy is the position of the antenna that is folded underneath the head, but a very similar condition is present in Coleorrhyncha, arguably a result of parallel evolution. A potential synapomorphy of Pentatomomorpha and Cimicomorpha is the absence of M19 (*M. transversalis labii primus*) (**70**) (Fig. 19A).

In MAHNER (1993), Nepomorpha are placed as the sister group of the remaining Heteroptera. A potential apomorphy of Heteroptera excluding Nepomorpha is the reduction of M29 (*M. dilatator postpharyngis ventralis*) (**69**) (Fig. 19B). This scenario appears less likely considering the number of steps and the implied character transformations.

XIE et al. (2008) suggested the monophyly of Euheteroptera as in WHEELER et al. (1993), but with Nepomorpha, instead of the Dipsocoromorpha, in a second basal position (Fig. 19C). Euheteroptera was supported by three potential apomorphies: the presence of distinct bucculae (**6**) (in agreement with the hypothesis of WHEELER et al. 1993), a reduced genal suture (**13**), and distinctly bi-lobed principal salivary glands (**51**).

Even though parsimony favors the pattern of WHEELER et al. (1993), with basal Enicocephalomorpha, and Dipsocoromorpha as the second branch, it is apparent that this issue is far from being settled. Apparently, morphological characters of the head are not sufficient for a reliable reconstruction of phylogenetic relationships of the major heteropteran lineages. The hemipteran head is highly derived, but main features are conserved within

the entire lineage and within the megadiverse Heteroptera. This is likely linked to the ubiquitous mechanism of liquid feeding and related functional constraints. Predacious feeding habits are presumably an apomorphic groundplan feature of Heteroptera and this has resulted in an entire series of cephalic character transformations, among them prognathism and the related presence of a gula and modified insertion of the labium (SWEET 1979). The ancestral feeding habits were largely maintained in the basal lineages, again resulting in more or less conserved cephalic structures. Evolutionary changes of cephalic features related with a switch to phytophagy may have played a role in the evolution of some of the “higher” heteropteran groups, i.e. the Pentatomomorpha and Cimicomorpha. An evaluation of this hypothesis is currently impeded by a severe lack of detailed morphological data.

What is apparently needed for a reliable phylogenetic reconstruction is more detailed morphological data, not only covering the head structures of a broader taxon sampling, but also features of the thorax and abdomen including the genitalia. This approach combined with extensive molecular data assembled in the 1KITE project (<http://www.1kite.org/>) and the hemipteroid AToL project (http://www.nsf.gov/awardsearch/showAward?AWD_ID=1239788&HistoricalAwards=false) will likely lead to a robust heteropteran phylogeny, which will be an ideal basis for developing a complex evolutionary scenario using well documented morphological (and palaeontological) information.

5. Acknowledgements

The authors are very grateful to Ralf Heckmann and Berend Aukema for providing valuable specimens of Dipsocoromorpha. Histological sections of exceptional quality were provided by Rommy Petersohn and Janin Naumann, which is also gratefully acknowledged.

6. References

- ANDERSEN N.M. 1982. The Semiaquatic Bugs (Hemiptera, Gerromorpha) – Phylogeny, Adaptations, Biogeography, and Classification. – *Entomograph* **3**: 1–455.
- AZAR D., NEL A. 2010. The earliest fossil schizopterid bug (Insecta: Heteroptera) in the Lower Cretaceous amber of Lebanon. – *Annales de la Société Entomologique de France* **46**(1–2): 193–197.
- BANAR P. 2008. A new species of *Systelloderes* (Hemiptera: Heteroptera: Enicocephalidae) from South Africa. – *Acta Entomologica Musei Nationalis Pragae* **48**(2): 233–240.
- BARTH R. 1952a. Estudos anatômicos e histológicos sobre a subfamília Triatominae (Heteroptera, Reduviidae). I. parte: A cabeça do *Triatoma infestans*. – *Memórias do Instituto Oswaldo Cruz* **50**: 70–155.
- BARTH R. 1952b. Anatomische und histologische Studien ueber die Unterfamilie Triatominae (Heteroptera, Reduviidae). I. Teil: Der Kopf von *Triatoma infestans*. – *Memórias do Instituto Oswaldo Cruz* **50**: 156–196.
- BARTH R. 1953a. Estudos anatômicos e histológicos sobre a subfamília Triatominae (Heteroptera, Reduviidae). III parte: Pesquisas sobre o mecanismo da picada dos Triatomina. – *Memórias do Instituto Oswaldo Cruz* **51**: 11–68.
- BARTH R. 1953b. Anatomische und histologische Studien ueber die Unterfamilie Triatominae (Heteroptera, Reduviidae). III. Teil: Untersuchungen ueber den Stechvorgang der Triatominae. – *Memórias do Instituto Oswaldo Cruz* **51**: 69–94.
- BENWITZ G. 1956. Der Kopf von *Corixa punctata* Ill. (*geoffroyi* Leach) (Hemiptera – Heteroptera). – *Zoologische Jahrbücher, Abteilung Anatomie* **75**: 311–378.
- BREMER K. 1994. Branch support and tree stability. – *Cladistics* **10**: 295–304.
- BROWN B.V. 1993. A further chemical alternative to critical-point-drying for preparing small (or large) flies. – *Fly Times* **11**: 10.
- CARVER M., GROSS G.F., WOODWARD T.E. 1991. Hemiptera (bugs, leafhoppers, cicadas, aphids, scale insects etc.). Pp. 429–509 in: NAUMANN I.D., CARNE P.B., LAWRENCE J.F., NIELSEN E.S., SPRADBERY J.P., TAYLOR R.W., WHITTEN M.J., LITTLEJOHN M.J. (eds.), *The Insects of Australia – A textbook for students and research workers*. 2nd edn., vol. 1. – Cornell University Press, Ithaca, New York.
- CASSIS G., SCHUH R.T. 2010. Systematic methods, fossils, and relationships within Heteroptera (Insecta). – *Cladistics* **26**: 262–280.
- CHINA W.E., MILLER N.C.E. 1959. Check-list and keys to the families and subfamilies of the Hemiptera-Heteroptera. – *Bulletin of the British Museum (Natural History)* **8**(1): 1–45.
- COBBEN R.H. 1968. Evolutionary Trends in Heteroptera. Part 1. Eggs, Architecture of the Shell, Gross Embryology and Ecdysis. – Centre for Agricultural Publications and Documentation, Wageningen, Nederland. 475 pp.
- COBBEN R.H. 1978. Evolutionary Trends in Heteroptera. Part 2: Mouthpart Structures and Feeding Strategies. – H Veeman and Zonen BV, Wageningen, Nederland. 407 pp.
- CRANSTON F.P., SPRAGUE I.B. 1961. A morphological study of the head capsule of *Gerris remigis* Say. – *Journal of Morphology* **108**(3): 287–309.
- DAMGAARD J. 2008. Evolution of the semi-aquatic bugs (Hemiptera: Heteroptera: Gerromorpha) with a re-interpretation of the fossil record. – *Acta Entomologica Musei Nationalis Pragae* **48**(2): 251–268.
- EMSLEY M.G. 1969. The Schizopteridae (Hemiptera: Heteroptera) with the description of a new species from Trinidad. – *Memoirs of the American Entomological Society* **25**: 1–154.
- FORBES A.R. 1977. The mouthparts and feeding mechanism of aphids. Pp. 83–103 in: HARRIS K. (ed.), *Aphids as Virus Vectors*. – Academic Press, New York.
- FRIEDRICH F., BEUTEL R.G. 2008. The thorax of *Zorotypus* (Hexapoda, Zoraptera) and a new nomenclature for the musculature of Neoptera. – *Arthropod Structure & Development* **37**: 29–54.
- GOLOBOFF P.A. 1999. NONA ver. 2. – Published by the author, Tucuman, Argentina.
- GOLOBOFF P.A., FARRIS J.S., NIXON K.C. 2003. TNT: tree analyses using new technology, program and documentation. – Available from <http://www.zmuc.dk/public/phylogeny>.
- GRAICHEN E. 1936. Das Zentralnervensystem von *Nepa cinerea* mit Einschluß des sympathischen Nervensystems. – *Zoologische Jahrbücher, Abteilung Anatomie* **61**: 195–238.
- GRIFFITH M.E. 1945. The environment, life history and structure of the water boatman, *Rhaphoeorixa acumznata* (Uhler) (Hemiptera, Corixidae). – *The University of Kansas Science Bulletin* **30**(11): 241–365.
- HAMILTON K.G.A. 1981. Morphology and evolution of the rhynchotan head (Insecta: Hemiptera, Homoptera). – *The Canadian Entomologist* **113**(11): 953–974.
- HAMILTON M.A. 1931. The morphology of the water-scorpion, *Nepa cinerea* Linn. (Rhynchota, Heteroptera). – *Proceedings of the Zoological Society of London* **3**: 1067–1136.
- HECKMANN R., RIEGER C. 2001. Wanzen aus Baden-Württemberg – Ein Beitrag zur Faunistik und Ökologie der Wanzen in Baden-Württemberg (Insecta, Heteroptera). – *Carolinae* **59**: 81–98.
- HENRY T.J. 2009. Biodiversity of Heteroptera. Pp. 223–263 in: FOOTITT R.G., ADLER P.H. (eds.), *Insect Biodiversity – Science and Society*. – Wiley-Blackwell, West Sussex, Oxford (UK).
- JORDAN K.H.C. 1972. 20. Heteroptera (Wanzen). Pp. 1–113 in: HELMCKE J.G., STARCK D., WERMUTH H. (eds), *Handbuch der Zoologie IV. Band: Arthropoda, 2. Hälfte: Insecta, 2. Teil Spezielles*. – Walter de Gruyter, Berlin.
- KÉLER VON S. 1963. Entomologisches Wörterbuch – mit besonderer Berücksichtigung der morphologischen Terminologie, 3rd edn. – Akademie-Verlag, Berlin.
- KHAN M.R. 1972. The anatomy of the head-capsule and mouthparts of *Dysdercus fasciatus* Sign. (Pyrrhocoridae, Hemiptera). – *Journal of Natural History* **6**: 289–310.

- KOPELKE J.P. 1978. Morphologische Charakteristika der Imagines von *Hydrocyrius columbiae columbiae* SPINOLA. – Deutsche Entomologische Zeitschrift N.F. **25**(1–3): 91–118.
- KRITSKY G. 1977. Observations on the morphology and behavior of the Enicocephalidae (Hemiptera). – Entomological News **88**(5,6): 105–110.
- KUMAR R. 1964. On some internal organs in Enicocephalidae, Lepidoptodidae and Ochteridae (Hemiptera). – Proceedings of the Royal Society of Queensland **75**(6): 39–44.
- KUMARI S. 1955. Studies on the morphology of the red cotton bug, *Dysdercus koenigii* Fabricius (Hemiptera: Pyrrhocoridae). Part I. External features and skeleto-muscular system of the head. – Journal of the Zoological Society of India **7**(2): 127–140.
- LESTON D., PENDERGRAST J.G., SOUTHWOOD T.R.E. 1954. Classification of the terrestrial Heteroptera (Geocorisae). – Nature **174**: 91–92.
- LI H., LIU H., SHI A., ŠTYS P., ZHOU X., CAI W. 2012a. The complete mitochondrial genome and novel gene arrangement of the unique-headed bug *Stenopirates* sp. (Hemiptera: Enicocephalidae). – PLoS ONE **7**(1): e29419. doi:10.1371/journal.pone.0029419.
- LI M., TIAN Y., ZHAO Y., BU W. 2012b. Higher level phylogeny and the first divergence time estimation of Heteroptera (Insecta: Hemiptera) based on multiple genes. – PLoS ONE **7**(2): e32152. doi:10.1371/journal.pone.0032152.
- LINDER H.J. 1956. Structure and histochemistry of the maxillary glands in the milkweed bug *Oncopeltus fasciatus* (Hem.). – Journal of Morphology **99**(3): 575–611.
- MAHNER M. 1993. Systema Cryptoceratorum Phylogenticum (Insecta, Heteroptera). – Zoologica **48**(143): 1–302.
- MATSUDA R. 1960. Morphology, evolution and a classification of the Gerridae (Hemiptera–Heteroptera). – University of Kansas Science Bulletin **41**: 25–632.
- MIYAMOTO S. 1961. Comparative morphology of alimentary organs of Heteroptera, with phylogenetic consideration. – Sieboldia **2**: 197–259.
- NIXON K.C. 2002. WinClada ver. 1.00.08. – Published by the author, Ithaca, NY.
- PARSONS M.C. 1958. Cephalic glands in *Gelastocoris* (Hemiptera–Heteroptera). – Psyche **65**: 99–107.
- PARSONS M.C. 1959. Skeleton and musculature of the head of *Gelastocoris oculatus* (Fabricius) (Hemiptera–Heteroptera). – Bulletin of the Museum of Comparative Zoology at Harvard College **122**(1): 3–53.
- PARSONS M.C. 1960a. Skeleton and musculature of the thorax of *Gelastocoris oculatus* (Fabricius). – Bulletin of the Museum of Comparative Zoology at Harvard College **122**(7): 299–357.
- PARSONS M.C. 1960b. The nervous system of *Gelastocoris oculatus* (Fabricius) (Hemiptera–Heteroptera). – Bulletin of the Museum of Comparative Zoology at Harvard College **123**(5): 131–199.
- PARSONS M.C. 1962. Skeleton and musculature of the head of *Saldula pallipes* (F.) Heteroptera: Saldidae. – Transactions of the Royal Entomological Society of London **114**(4): 97–130.
- PARSONS M.C. 1963. Thoracic skeleton and musculature of adult *Saldula pallipes* (F.) Heteroptera: Saldidae. – Transactions of the Royal Entomological Society of London **115**(1): 1–37.
- PARSONS M.C. 1968. The cephalic and prothoracic skeleto-musculature and nervous system in *Lethocerus* (Heteroptera, Belostomatidae). – Journal of the Linnean Society (Zoology) **47**(312): 349–406.
- POHL H. 2010. A scanning electron microscopy specimen holder for viewing different angles of a single specimen. – Microscopy Research and Technique **73**(12): 1073–1076.
- REUTER O.M. 1910. Neue Beiträge zur Phylogenie und Systematik der Miriden nebst einleitenden Bemerkungen über die Phylogenie der Heteropteren-Familien. – Acta Societatis Scientiarum Fennicae **37**(3): 1–171.
- RIEGER C. 1976. Skelett und Muskulatur des Kopfes und Prothorax von *Ochterus marginatus* Latreille. – Zoomorphologie **83**: 109–191.
- SAXENA P.N., CHADA H.L. 1971. The greenbug, *Schizaphis graminum*. 2. The salivary gland complex. – Annals of the Entomological Society of America **64**(4): 904–912.
- SCHUH R.T. 1979. [Review of] Evolutionary trends in Heteroptera. Pt. 2. Mouthpart-structures and feeding strategies. – Systematic Zoology **28**(4): 653–656.
- SCHUH R.T. 1986. The influence of cladistics on heteropteran classification. – Annual Review of Entomology **31**: 67–93.
- SCHUH R.T., ŠTYS P. 1991. Phylogenetic analysis of cimicomorphan family relationships (Heteroptera). – Journal of the New York Entomological Society **99**(3): 298–350.
- SCHUH R.T., SLATER J.A. 1995. True Bugs of the World (Hemiptera: Heteroptera) – Classification and Natural History. – Cornell University Press, New York. 337 pp.
- SHCHERBAKOV D.E., POPOV Y.A. 2002. Superorder Cimicidea Laicharting, 1781. Order Hemiptera Linné, 1758. The Bugs, Cicadas, Plantlice, Scale Insects, etc. (= Cimicida Laicharting, 1781, = Homoptera Leach, 1815 + Heteroptera Latreille, 1810). Pp. 143–157 in: RASNITSYN A.P., QUICKE D.L.J. (eds), History of Insects. – Kluwer Academic Publishers, Dordrecht, Boston, London.
- SINGH S. 1971. Morphology of the head of Homoptera. – Research Bulletin of the Panjab University **22**(3–4): 261–316.
- SPANGENBERG R., WIPLER B., FRIEDEMANN K., POHL H., WEIRAUCH C., HARTUNG V., BEUTEL R.G. 2013. The cephalic morphology of the Gondwanan key taxon *Hackeriella* (Coleorrhyncha, Hemiptera). – Arthropod Structure & Development **42**: 315–337.
- SPOONER C.S. 1938. The phylogeny of Hemiptera based on a study of the head capsule. – Illinois Biological Monographs **16**(3): 1–102.
- SPRAGUE I.B. 1956. The biology and morphology of *Hydrometra martini* Kirkaldy. – The University of Kansas Science Bulletin **38**(9): 579–693.
- ŠTYS P. 1970. On the morphology and classification of the family Dipsocoridae s. lat., with particular reference to the genus *Hysipteryx* Drake (Heteroptera). – Acta Entomologica Bohemoslovaca **67**: 21–46.
- ŠTYS P. 1983. A new family of Heteroptera with dipsocoromorphan affinities from Papua New Guinea. – Acta Entomologica Bohemoslovaca **80**: 256–292.
- ŠTYS P. 1984. [Abstract of] Plural origin of the male intromittent organ in Heteroptera. – 17th International Congress of Entomology, Hamburg.
- ŠTYS P. 1995a. 11. Enicocephalomorpha. P. 67 in: SCHUH R.T., SLATER J.A. (eds.), True Bugs of the World (Hemiptera: Heteroptera) – Classification and Natural History. – Cornell University Press, New York.

- ŠTYS P. 1995b. 14. Dipsocoromorpha. Pp. 74–75 in: SCHUH R.T., SLATER J.A. (eds.), True Bugs of the World (Hemiptera: Heteroptera) – Classification and Natural History. – Cornell University Press, New York.
- ŠTYS P. 1995c. 15. Ceratocombidae. Pp. 75–78 in: SCHUH R.T., SLATER J.A. (eds.), True Bugs of the World (Hemiptera: Heteroptera) – Classification and Natural History. – Cornell University Press, New York.
- ŠTYS P. 1995d. 16. Dipsocoridae. Pp. 78–79 in: SCHUH R.T., SLATER J.A. (eds.), True Bugs of the World (Hemiptera: Heteroptera) – Classification and Natural History. – Cornell University Press, New York.
- ŠTYS P. 1995e. 17. Schizopteridae. Pp. 80–82 in: SCHUH R.T., SLATER J.A. (eds.), True Bugs of the World (Hemiptera: Heteroptera) – Classification and Natural History. – Cornell University Press, New York.
- ŠTYS P. 2008. Zoogeography of Enicocephalomorpha (Heteroptera). – *Bulletin of Insectology* **61**(1): 137–138.
- ŠTYS P., BANAR P. 2008. *Xenicocephalus* – an enigmatic genus of American Enicocephalidae (Heteroptera): a new male-based species from Suriname. Pp. 357–376 in: GROZEVA S., SIMOV N. (eds.), *Advances in Heteroptera Research, Festschrift in Honour of 80th Anniversary of Michail Josifov*.
- ŠTYS P., KERZHNER I. 1975. The rank and nomenclature of higher taxa in recent Heteroptera. – *Acta Entomologica Bohemoslovaca* **72**: 65–79.
- ŠTYS P., BANAR P., DRESCHER J. 2010. A new *Oncyclocotis* Stål (Hemiptera: Heteroptera: Enicocephalidae) from Sabah: a predacious species associated with the yellow crazy ant, *Anoplolepis gracilipes* (Smith) (Hymenoptera: Formicidae). – *Zootaxa* **2651**: 27–42.
- SWART C.C., FELGENHAUER B.E. 2003. Structure and function of the mouthparts and salivary gland complex of the giant waterbug, *Belostoma lutarium* (Stål) (Hemiptera: Belostomatidae). – *Annals of the Entomological Society of America* **96**(6): 870–882.
- SWEET M.H. 1979. On the original feeding habits of the Hemiptera (Insecta). – *Annals of the Entomological Society of America* **72**(5): 575–579.
- USINGER R.L. 1932. Miscellaneous studies in the Henicocephalidae (Hemiptera). – *The Pan-Pacific Entomologist* **8**(4): 145–156.
- USINGER R.L. 1945. Classification of the Enicocephalidae (Hemiptera, Reduvioidea). – *Annals of the Entomological Society of America* **38**: 321–342.
- USINGER R.L., WYGODZINSKY P.W. 1960. Heteroptera: Enicocephalidae. – *Insects of Micronesia* **7**(5): 219–230.
- VERMA S.R., TYAGI M.P., GUPTA S.P. 1973. Studies on the morphology of *Belostoma indicus* Lep. et. Serv. (head capsule and mouth parts). – *Zoologische Jahrbücher, Anatomie* **91**: 449–463.
- WEBER H. 1928. Skelett, Muskulatur und Darm der schwarzen Blattlaus *Aphis fabae* Scop. – *Zoologica* **76**: 1–130.
- WEBER H. 1929. Zur vergleichenden Physiologie der Saugorgane der Hemipteren – mit besonderer Berücksichtigung der Pflanzenläuse. – *Zeitschrift für Vergleichende Physiologie* **8**: 145–186.
- WEIRAUCH C. 2008. From four- to three-segmented labium in Reduviidae (Hemiptera: Heteroptera). – *Acta Entomologica Musei Nationalis Pragae* **48**(2): 331–344.
- WEIRAUCH C. 2012. *Voragocoris schuhi*, a new genus and species of neotropical Schizopterinae (Hemiptera: Heteroptera: Schizopteridae). – *Entomologica Americana* **118**(1–4): 285–294.
- WEIRAUCH C., CASSIS G. 2009. Frena and druckknopf: a synopsis of two forewing-to-body coupling mechanisms in Heteropteroidea (Hemiptera). – *Insect Systematics and Evolution* **40**: 229–252.
- WEIRAUCH C., SCHUH R.T. 2011. Systematics and evolution of Heteroptera: 25 years of progress. – *Annual Review of Entomology* **56**: 487–510.
- WEIRAUCH C., ŠTYS P. in press. Litter bugs exposed – phylogenetic relationships of Dipsocoromorpha (Hemiptera: Heteroptera) based on molecular data. – *Insect Systematics and Evolution*.
- WHEELER W.C., SCHUH R.T., BANG R. 1993. Cladistic relationships among higher groups of Heteroptera: congruence between morphological and molecular data sets. – *Entomologica Scandinavica* **24**: 121–137.
- WIPLER B., MACHIDA R., MÜLLER B., BEUTEL R.G. 2011. On the head morphology of Grylloblattodea (Insecta) and the systematic position of the order, with a new nomenclature for the head muscles of Dicondylia. – *Systematic Entomology* **36**: 241–266.
- WYGODZINSKY P.W., SCHMIDT K. 1991. Revision of the new world Enicocephalomorpha (Heteroptera). – *Bulletin of the American Museum of Natural History* **200**: 1–265.
- XIE Q., TIAN Y., ZHENG L., BU W. 2008. 18S rRNA hyper-elongation and the phylogeny of Euhemiptera (Insecta: Hemiptera). – *Molecular Phylogenetics and Evolution* **47**: 463–471.
- YANG C.T. 2002. Preliminary thoughts on the phylogeny of Coleorrhyncha–Heteroptera (Hemiptera). – *Formosan Entomologist* **22**: 297–305.
- YOSHIZAWA K., SAIGUSA T. 2001. Phylogenetic analysis of paraneopteran orders (Insecta: Neoptera) based on forewing base structure, with comments on monophyly of Auchenorrhyncha (Hemiptera). – *Systematic Entomology* **26**: 1–13.
- ZRZAVÝ J. 1990. Evolution of antennal sclerites in Heteroptera (Insecta). – *Acta Universitatis Carolinae – Biologica* **34**: 189–227.